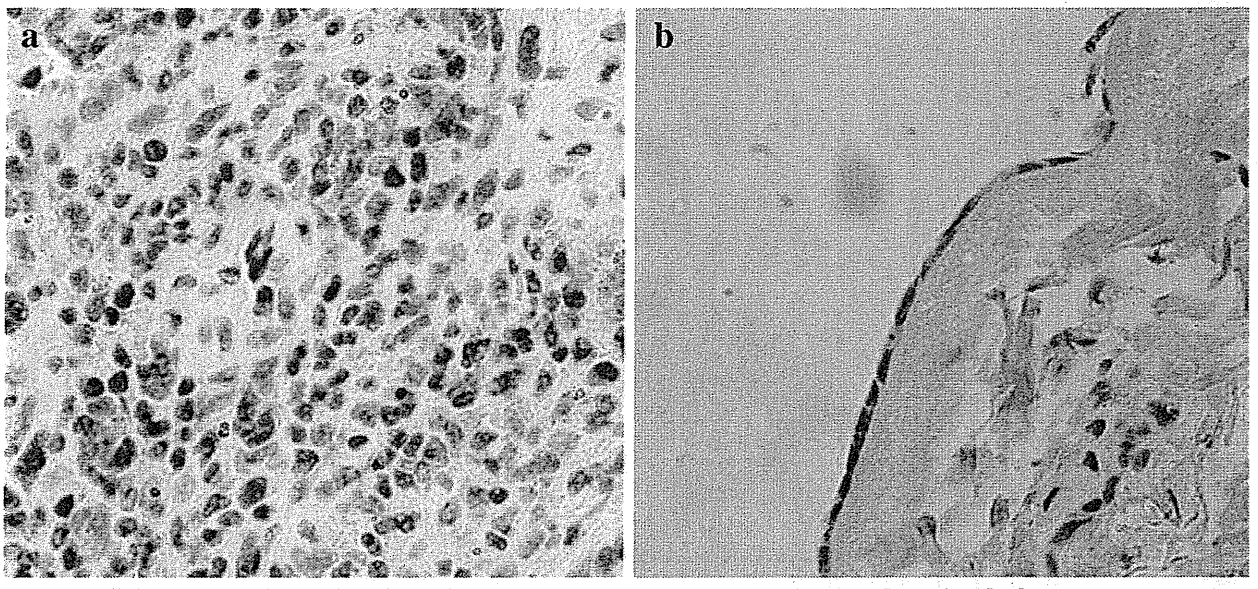

FIG. 6.

ZEB1 protein is expressed in a substantial fraction of human MPM tissue sections. Representative photographs of immunohistochemical staining of ZEB1 in MPM tumor (**a**) and normal parietal pleural (**b**) tissue sections. Original magnification, ×400

TABLE 1

More than 4-fold up-regulated genes by transient *ZEB1* knockdown in ACC-MESO-1 cells

	Transient knockdown		Stable knockdown		Gene neame
Symbol	**Fold**	**Log2**	**Fold**	**Log2**	
EPCAM	17.6	4.1	115.8	6.9	Epithelial cell adhesion molecule
SPINT2	6.2	2.6	2.4	1.3	serine peptidase inhibitor, Kunitz type, 2
CDS1	6.1	2.6	5.1	2.4	CDP-diacylglycerol synthase 1
F2RL1	5.3	2.4	2.7	1.4	coagulation factor II (thrombin) receptor-like 1
DDIT4	5.3	2.4	4.6	2.2	DNA-damage-inducible transcript 4
IGSF6	5.3	2.4	[illegible]	2.9	immunoglobulin superfamily, member 6
PDE1C	4.9	2.3	0.9	−0.2	phosphodiesterase 1C, calmodulin-dependent 70kDa
ARL15	4.7	2.2	[illegible]	2.0	ADP-ribosylation factor-like 15
TJP3	4.7	2.2	0.5	−0.9	tight junction protein 3 (zona occludens 3)
RNASEN	4.6	2.2	0.0		drosha, ribonuclease type III
GRB14	4.5	2.2	7.4	2.9	growth factor receptor-bound protein 14
APOC2	4.4	2.1	0.7	−0.5	apolipoprotein C-II
SERPINI1	4.3	2.1	2.0	1.0	serpin peptidase inhibitor, clade I (neuroserpin), member 1
CLTCL1	4.3	2.1	1.3	0.4	clathrin, heavy chain-like 1
BCL7A	4.1	2.0	1.0	0.0	B-cell CLL/lymphoma 7A
AIF1L	4.0	2.0	1.0	0.0	allograft inflammatory factor 1-like
ADAMTS1	4.0	2.0	1.8	0.8	ADAM metallopeptidase with thrombospondin type 1 motif, 1

Expression change (log2) ≤−2.0 ≤−1.0 −1.0> <1.0 ≥1.0 ≥2.0

Ann Surg Oncol. Author manuscript; available in PMC 2012 August 08.

TABLE 2

More than 4-fold down-regulated genes by transient *ZEB1* knockdown in ACC-MESO-1 cells

	Transient knockdown		Stable knockdown		Gene neame
Symbol	**Fold**	**Log2**	**Fold**	**Log2**	
TMEM30A	0.10	−3.2	0.8	−0.2	transmembrane protein 30A
SLC25A15	0.13	−2.9	0.8	−0.3	solute carrier family 25 member 15
APPL	0.14	−2.8	1.6	0.6	adaptor protein, phosphotyrosine interaction, PH domain and leucine Zipper
SLC4A8	0.15	−2.8	0.3	−1.7	solute carrier family 4, sodium bicarbonate cotransporter, member 8
STYX	0.16	−2.6	1.3	0.4	serine/threonine/tyrosine interacting protein
CAV1	0.17	−2.6	0.8	−0.3	caveolin 1, caveolae protein, 22kDa
ACADM	0.18	−2.5	0.5	−1.0	acyl-CoA dehydrpgenase, C-4 to C-12 straight chain
GJA1	0.18	−2.5	0.3	−1.6	gap junction protein, alpha 1, 43kDa
C13orf37	0.19	−2.4	1.0	0.0	mitotic spindle organizing protein 1
NXT2	0.19	−2.4	0.7	−0.6	nuclear transport factor 2-like export factor 2
MAPRE1	0.20	−2.3	1.1	0.2	microtubule-associated protein, RP/EB family, member 1
CRYBA4	0.22	−2.2	0.0		crystallin, beta A4
VMA21	0.23	−2.1	0.5	−1.0	VMA21 vacuolar H+ATpase homolog (S. cerevisiae)
ZEB1	0.23	−2.1	0.2	−2.0	zinc finger E-box binding homeobox 1
NLRP1	0.24	−2.1	0.6	−0.7	NLR family, pyrin domain containing 1
NSF	0.24	−2.0	0.6	−0.8	N-ethylmaleimide-sensitive factor
DMD	0.25	−2.0	1.2	0.3	dystrophin
MPP4	0.25	−2.0	0.0		membrane protein, palmitoylated 4 (MAGUK p55 subfamily member 4)
CMTM6	0.25	−2.0	0.8	−0.4	CKLF-like MARVEL transmembrane domain containing 6

Expression change (log2) ≤−2.0 | <−1.0 | −1.0> <1.0 | ≥1.0 | ≥2.0

Oncogene (2012) **31,** 5117–5122

www.nature.com/onc

SHORT COMMUNICATION

YAP induces malignant mesothelioma cell proliferation by upregulating transcription of cell cycle-promoting genes

T Mizuno[1,2], H Murakami[1], M Fujii[1], F Ishiguro[1,2], I Tanaka[1], Y Kondo[1], S Akatsuka[3], S Toyokuni[3], K Yokoi[2], H Osada[1,4] and Y Sekido[1,4]

Malignant mesothelioma (MM) shows frequent inactivation of the *neurofibromatosis type 2* (*NF2*) –tumor-suppressor gene. Recent studies have documented that the Hippo signaling pathway, a downstream cascade of Merlin (a product of *NF2*), has a key role in organ size control and carcinogenesis by regulating cell proliferation and apoptosis. We previously reported that MMs show overexpression of *Yes-associated protein* (YAP) transcriptional coactivator, the main downstream effector of the Hippo signaling pathway, which results from the inactivation of *NF2*, *LATS2* and/or *SAV1 genes* (the latter two encoding core components of the mammalian Hippo pathway) or amplification of *YAP* itself. However, the detailed roles of YAP remain unclear, especially the target genes of YAP that enhance MM cell growth and survival. Here, we demonstrated that YAP-knockdown inhibited cell motility, invasion and anchorage-independent growth as well as cell proliferation of MM cells *in vitro*. We analyzed genes commonly regulated by YAP in three MM cell lines with constitutive YAP-activation, and found that the major subsets of YAP-upregulating genes encode cell cycle regulators. Among them, YAP directly induced the transcription of *CCND1* and *FOXM1*, in cooperation with TEAD transcription factor. We also found that knockdown of *CCND1* and *FOXM1* suppressed MM cell proliferation, although the inhibitory effects were less evident than those of YAP knockdown. These results indicate that constitutive YAP activation in MM cells promotes cell cycle progression giving more aggressive phenotypes to MM cells.

Oncogene (2012) **31,** 5117–5122; doi:10.1038/onc.2012.5; published online 30 January 2012

Keywords: malignant mesothelioma; Hippo pathway; YAP; CCND1; cell cycle

INTRODUCTION

Malignant mesothelioma (MM) is one of the most aggressive neoplasms, which is caused by asbestos exposure.[1,2] It is usually resistant to conventional therapies, and the prognosis of patients is very poor. The median survival of malignant pleural mesothelioma patients after diagnosis is 7–11 months.[1,3,4] There is a 30–40 year interval before clinical presentation of the tumor after asbestos exposure.[5] While the long latency of the disease implies that multiple genetic and epigenetic alterations might be required for MM progression,[6] the detailed molecular pathogenesis of MM has not been well understood.

Among the limited number of genes that are frequently mutated in MMs, inactivation of $p16^{INK4a}/p14^{ARF}$ is detected in over 70% of MMs.[7] The *NF2* gene, which is responsible for the *NF2* familial cancer syndrome, has been shown to be inactivated in 40–50% of MMs.[8,9] A recent study has also indicated that 23% of MM cases had an inactivating mutation of *BAP1*, which encodes a nuclear deubiquitinase.[10,11]

The *NF2* gene encodes Merlin, which is a membrane-cytoskeleton-associated protein with four-point-one, ezrin, radixin and moesin domain, and acts as a tumor suppressor.[12] One of the downstream signaling cascades regulated by Merlin is the Hippo signaling pathway, which is conserved from *Drosophila* to mammalians.[13–15] In MM cells, besides the *NF2* mutation, genetic alterations in the components of the Hippo signaling pathway have also been identified recently, including inactivating mutations of *large tumor suppressor 1* (*LATS1*), *LATS2* and *SAV1*, and amplification of *Yes-associated protein* (*YAP*).[10,16,17] Together with *NF2* mutation, MM shows frequent Merlin-Hippo pathway inactivation, which leads to YAP activation in over 70% of MM cases.[18]

Studies have shown that the Hippo signaling pathway is involved in the cell cycle regulation and the control of organ size.[19,20] The dysregulation of this pathway, which leads to constitutive YAP activation, induces the oncogenic transformation in cooperation with distinct transcription factors such as TEAD family members.[21–24] Overexpression, especially dominant expression in the nuclei compared with the cytoplasm of tumor cells and the oncogenic roles of YAP have been shown in various types of human malignancies.[25–29] On the other hand, the anti-proliferative or apoptosis-inducing function of YAP has also been demonstrated in the context of DNA damage or cellular stress, which induces its binding of YAP with other transcription factors such as p73, a paralog of p53 tumor suppressor.[30–32]

We previously showed that YAP promoted cell proliferation[17] and exogenous LATS2 inhibited cell proliferation via induction of YAP phosphorylation in MM cells.[16] However, the detailed characteristics of YAP oncogenic properties remain unclear, including the exact target genes that are inducible by YAP activation in MM cells. In this study, we aimed to identify the target genes of YAP in MM cells to elaborate how YAP induces the MM-cell malignant phenotypes. We found that cell cycle-regulating genes, including *CCDN1* and *FOXM1*, are induced by YAP, suggesting that the dysregulation of cell cycle regulation is one of the key alterations in which MM cells acquire malignancy by YAP activation.

[1]Division of Molecular Oncology, Aichi Cancer Center Research Institute, Nagoya, Japan; [2]Department of Thoracic Surgery, Nagoya University Graduate School of Medicine, Nagoya, Japan; [3]Department of Pathology and Biological Responses, Nagoya University Graduate School of Medicine, Nagoya, Japan and [4]Department of Cancer Genetics, Program in Function Construction Medicine, Nagoya University Graduate School of Medicine, Nagoya, Japan. Correspondence: Dr Y Sekido, Division of Molecular Oncology, Aichi Cancer Center Research Institute, Kanokoden 1-1, Chikusa-ku, Nagoya, Aichi 464-8681, Japan. E-mail: ysekido@aichi-cc.jp
Received 3 September 2011; revised 19 December 2011; accepted 30 December 2011; published online 30 January 2012

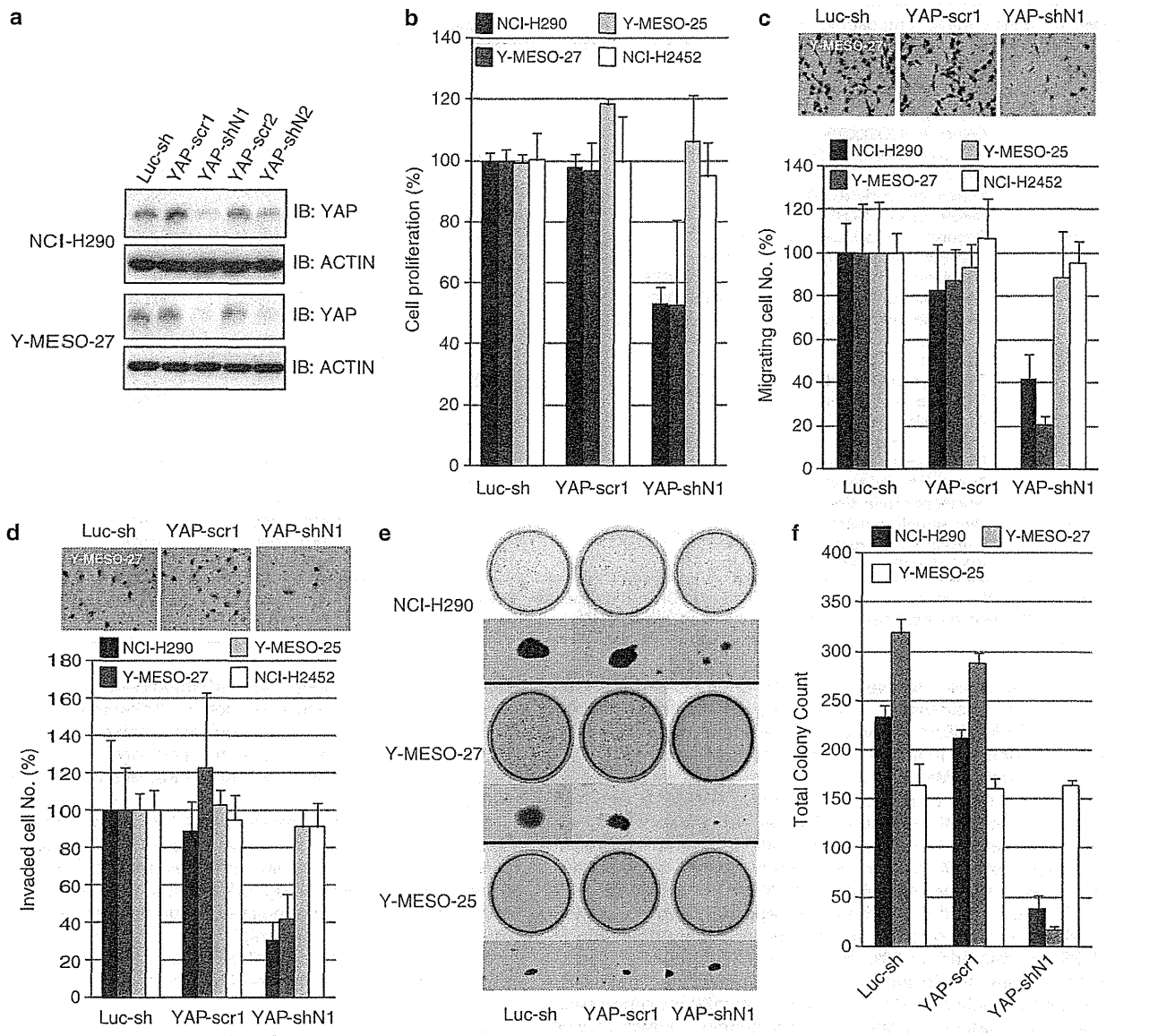

Figure 1. YAP knockdown suppressed malignant phenotypes of MM cell lines with YAP activation (NCI-H290 and Y-MESO-27) but not of those without YAP activation (Y-MESO-25 and NCI-H2452). (**a**) Western blot analyses for knockdown efficacies of short hairpin (sh)-YAP RNA interference lentivirus vectors. Two sh-YAP RNA interference lentivirus vectors (YAP-shN1 and YAP-shN2) contained each target sequence of YAP. Control shRNA vectors for luciferase (Luc-sh) with the target sequence for luciferase and for YAP (YAP-scr1 and YAP-scr2) with each scrambled target sequence were also constructed. Total cell lysates were subjected to western blot analysis using rabbit anti-YAP antibody and mouse anti-β-actin antibody. YAP-shN1 induced more potent YAP suppression compared with YAP-shN2. (**b**) Cell proliferation assay. After 72 h of lentivirus infection, calorimetric assays were performed with Tetra Color One (Seikagaku, Tokyo, Japan) and absorbance was measured at 450 nm. Cell proliferations were reduced to approximately 50% with YAP knockdown in NCI-H290 and Y-MESO-27 cell lines. (**c**) Migration assay. Cell migration and invasion potential were measured by *in vitro* Boyden chamber assays (BD Biosciences Discovery Labware, Bedford, MA, USA). Upper photographs show representative images of the migrating Y-MESO-27 cells. (**d**) Invasion assay. Matrigel matrix insert membrane was used for invasion assay. Upper photographs show representative images of invading Y-MESO-27 cells. (**e**) Soft agar colony formation assays. After a 10 day-incubation, colonies were stained with 0.3% crystal violet. Photographs of low (top) and high magnification (bottom) show that anchorage-independent growth was significantly suppressed with YAP knockdown in NCI-H290 and Y-MESO-27 but not Y-MESO-25 cell line. (**f**) A graphic presentation of the soft agar colony formation assays of (**e**). Columns are the means of experiments, and bars represent s.d. (**b**, **c**, **d**, **f**).

RESULTS AND DISCUSSION

Knockdown of YAP suppressed oncogenic properties of MM cells

We previously reported that several MM cell lines with *NF2* and/or *LATS2* mutations have constitutive YAP activation with low-level phosphorylation of YAP (S127).[16] Using western blot analysis with a panel of 23 MM cell lines, we confirmed that 16 (70%) cell lines showed lower levels of pYAP-S127 than MeT-5A, a transformed normal mesothelial cell line (Supplementary Figure 1). Among them, we selected three MM cell lines with constitutive YAP activation for further analyses; NCI-H290 with *NF2* inactivation, and Y-MESO-27 and Y-MESO-30 with *LATS2* inactivation.

Table 1. Gene ontology and pathway analyses in 228 genes commonly downregulated by YAP knockdown

Rank	*Name*	*Score*	*Score (p)*	*Score (v)*	*Score (c)*
(a) *Top 10 Gene ontology*					
1	Cell cycle (GO:0007049)	137.598	3.791E−042	0.409	0.079
2	Cell cycle process (GO:0022402)	129.250	1.235E−039	0.358	0.090
3	Cell cycle phase (GO:0022403)	117.627	3.897E−036	0.302	0.105
4	Mitotic cell cycle (GO:0000278)	107.258	5.153E−033	0.289	0.097
5	Mitotic phase (GO:0000279)	90.202	7.021E−028	0.214	0.124
6	Regulation of cell cycle (GO:0051726)	86.379	9.939E−027	0.264	0.080
7	Organelle organization (GO:0006996)	82.447	1.517E−025	0.371	0.047
8	Regulation of cell cycle process (GO:0010564)	80.848	4.596E−025	0.176	0.147
9	Regulation of metabolic process (GO:0019222)	76.863	7.275E−024	0.528	0.029
10	Regulation of cellular metabolic process (GO:0031323)	71.798	2.435E−022	0.491	0.030
(b) *Top 10 gene pathway*					
1	Transcriptional regulation by RB/E2F	297.728	2.371E−090	0.234	0.207
2	Transcriptional regulation by FOXM	63.604	7.135E−020	0.043	0.360
3	Aurora signaling pathway	52.246	1.872E−016	0.038	0.258
4	CDK signaling pathway	46.256	1.190E−014	0.043	0.107
5	PLK signaling pathway	45.168	2.531E−014	0.033	0.241
6	Transcriptional regulation by AP-1	35.712	1.777E−011	0.038	0.067
7	Nucleophosmin signaling pathway	29.087	1.753E−009	0.024	0.152
8	Wnt signaling pathway	28.376	2.870E−009	0.029	0.076
9	Transcriptional regulation by Myb	27.041	7.242E−009	0.029	0.065
10	PIN1 signaling pathway	22.329	1.898E−007	0.024	0.061

Abbreviations: AP-1, adaptor-related protein complex 1; CDK, cyclin-dependent kinase; FOXM, forkhead box M; Myb, v-myb myeloblastosis viral oncogene homolog; PIN, peptidylprolyl cis/trans isomerase NIMA-interacting 1; PLK, polo-like kinase; RB/E2F, retinoblastoma/E2F transcription factor.

As we previously showed that YAP inhibition suppressed NCI-H290 cell proliferation,[17] we first confirmed that a newly established YAP-shRNA lentivirus more efficiently suppressed the YAP expression and inhibited the cell proliferation of NCI-H290 cell line and another MM cell line, Y-MESO-27, which had *LATS2* deletion, but not in two other MM cell lines, Y-MESO-25 and NCI-H2452, without YAP activation (Figures 1a and b). Next, we analysed whether YAP knockdown affected other malignant phenotypes of MM cells *in vitro*. Both motility and invasive abilities were significantly inhibited in NCI-H290 and Y-MESO-27 cells (Figures 1c and d). Anchorage-independent growth analysis revealed a nearly complete suppression of colony formation in Y-MESO-27 cells and an 80% decrease in NCI-H290 cells (Figures 1e and f). These results indicate that YAP suppression in MM cells with constitutively activated YAP induces significant suppression of motility, invasion and anchorage-independent growth as well as cell proliferation *in vitro*.

Identification of YAP-regulating genes by microarray-based expression profiling analysis

As for the target genes of YAP orthologs, *cyclin E, Diap1* and *bantam* microRNA have been identified for *Drosophila Yokie*.[19] For mammalian YAP, although several genes including the *connective tissue growth factor* (*CTGF*) gene were shown as direct target genes of YAP,[24] other possible candidate target genes for mammalian counterparts do not seem to be really substantiated yet or even excluded, implying that YAP target genes vary among different species as well as among different cell types.

To identify the genes inducible for expression by YAP and responsible for MM cell proliferation, we performed microarray-based expression profiling analysis of the three MM cell lines after YAP knockdown. We found that 1381, 650 and 2097 genes were downregulated to equal or less than 0.5 in the NCI-H290, Y-MESO-27 and Y-MESO-30 cells, respectively, compared with each counterpart cell with the control vector (data not shown). We found that 228 genes were commonly downregulated by YAP knockdown, suggesting that this gene set includes strong candidates for YAP target genes in MM cells (Supplementary Table 1). To characterize the 228 genes, we performed gene ontology analysis and found that the large portion of YAP-regulatory genes is associated with cell cycle regulation (Table 1). Subsequent pathway analysis revealed that the pathways of transcriptional regulation by *RB/E2F* and *FOXM* were most significantly correlated (Table 1).

Meanwhile, our results revealed that 156 genes were commonly upregulated after YAP knockdown over twofold (Supplementary Table 1). Gene ontology and pathway analyses indicated that genes involved in wounding, inflammation and cell–extracellular matrix adhesion were upregulated, suggesting that suppression of these signaling pathways might also contribute to malignant phenotypes of MM cells by YAP activation, albeit their expressions might be indirectly suppressed (Supplementary Table 2).

YAP regulates CCND1 and FOXM1 transcription directly in cooperation with TEAD

Among the identified cell cycle regulatory genes, we focused on *CCND1*, a G1 cyclin-regulating RB/E2F pathway, and *FOXM1*, a transcription factor targeting both G1/S and G2/M progression regulators. *CCND1* and *FOXM1* were found to be commonly downregulated in the three cell lines from 0.13 to 0.48 and from 0.13- to 0.42-changes, respectively (Supplementary Table 1). Moreover, their promoter regions were also likely to harbor a putative recognition motif of TEAD, a transcriptional factor that binds to YAP.

To determine whether YAP regulates transcription of *CCND1* and *FOXM1* directly in MM cells, we carried out a chromatin immunoprecipitation assay. We prepared a primer set for the proximal promoter region of both genes to include the putative TEAD recognition motif[33] (Figure 2a). When precipitated with anti-YAP antibody, we detected positive PCR products of the proximal promoter regions of both genes, which indicated the direct binding of YAP to the *CCND1* and *FOXM1* proximal promoter regions (Figure 2b), although they were not detected in the distal regions (data not shown).

Next, to determine whether YAP induces transcription of *CCND1* and *FOXM1*, and then transcription is further enhanced

by exogenous TEAD transcription factor, we performed luciferase reporter assay for the promoter regions of these genes (Figure 2a) with YAP wild type and its constitutively active form, YAP S127A. We found that cotransduction of wild-type TEAD4 with YAP wild type or the active mutant form significantly induced both *CCND1* and *FOXM1* promoter activities. On the other hand, cotransduction of other mutant forms including YAP S94A[24] or TEAD4ΔCt,[34] both of which were thought to disrupt the YAP-TEAD interaction, did not show the enhancement of luciferase activity (Figures 2c and d).

These results provided support for the notion that *CCND1* and *FOXM1* might be the direct target genes of YAP in MM cells. Consistent with our observations, induction of *CCND1* by YAP has also been suggested by other studies. For example, in vertebrate neural tube development, YAP and TEAD promoted cell cycle progression by inducing *CCND1*.[21] As an upstream suppressive regulator of YAP, Merlin was also shown to inhibit *CCND1* expression by using *NF2*-deficient MM cells.[35] Although those reports did not refer to transcriptional regulation of *CCND1* by YAP, they demonstrated a contribution of Hippo signaling pathway to *CCND1* regulation, which our present findings corroborate.

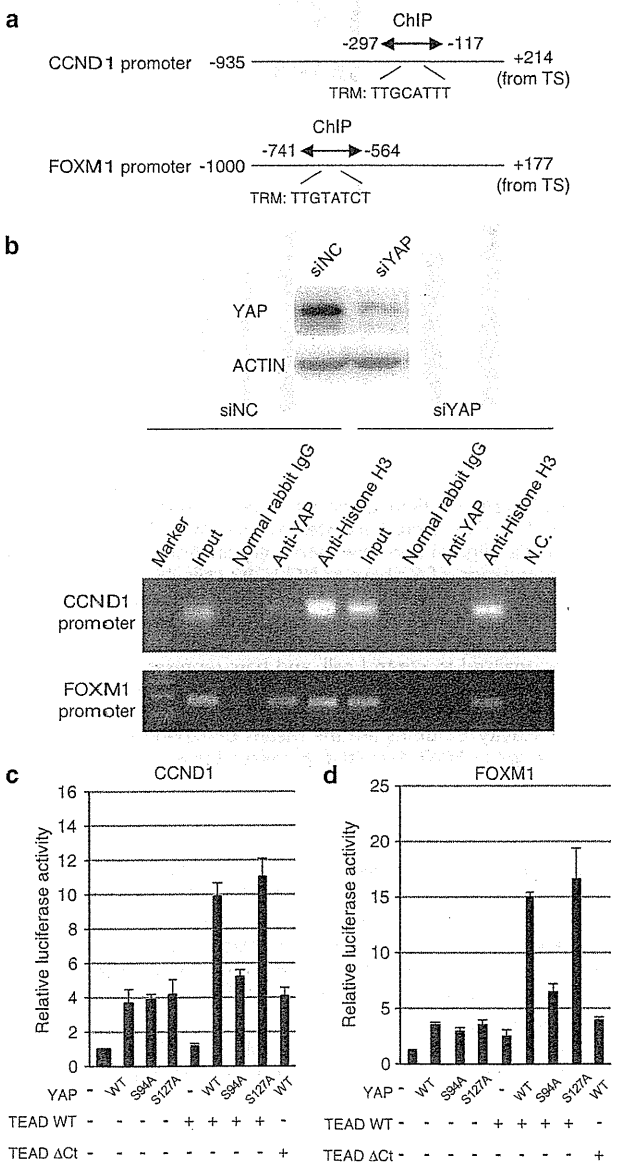

Figure 2. YAP directly induces transcription of the *CCND1* and *FOXM1* genes. (**a**) Each promoter includes the putative TEAD recognition motif (TRM), XDGHATXT, where X = A, T, C or G; D = A or T; and H = A, T or C. ChIP primer sets (arrow) were designed to include the motif. DNA fragments of nucleotide position −935 to +214 for *CCND1* and nucleotide position −1000 to +177 for *FOXM1* were inserted into luciferase reporter vectors. TS: transcriptional start. (**b**) ChIP assay using ChIP kit (ab500, Abcam) demonstrated that YAP bound to the *CCND1* and *FOXM1* proximal promoter regions. NCI-H290 cells treated with YAP siRNA (siYAP; Ambion, Austin, TX) were used as YAP-suppressed control, while cells with an irrelevant siRNA (siNC) maintained high YAP expression, as confirmed with western blot analysis. (Upper panel) After the cells with high or low YAP expression were subjected to immunoprecipitation assay with normal rabbit IgG (SC2027, Santa Cruz), rabbit anti-YAP antibody, or anti-H3 antibody (ab1791, Abcam) and protein A beads, immunoprecipitated chromatin were decross-linked. Recruited DNA was subjected to PCR using primer sets for proximal promoter regions of *CCND1* and *FOXM1*, and PCR products were electrophoresed in agarose gel. (Lower panel) Note that amounts of PCR products from the chromatin, which was precipitated with the anti-YAP antibody, were suppressed by pretreatment with siYAP. (**c, d**) For reporter assay, MeT-5A cells were transfected with the pGL3 basic firefly luciferase reporter plasmid with the *CCND1* or *FOXM1* promoter region by using FuGENE 6 transfection reagent (Roche, Mannheim, Germany). Renilla luciferase plasmid was also transfected for internal control. Thirty-six hours later, cells were lysed and subjected to dual-luciferase assay (TOYO INK, Tokyo, Japan). The promoter activities were enhanced with combined transduction of TEAD4 WT with wild type (WT) or constitutively activated forms of YAP (YAP S127A), but not with YAP S94A (inactive for TEAD binding) or TEAD4ΔCt (inactive for YAP binding) forms. Columns are the means of experiments, and bars represent s.d. (**c, d**).

YAP depletion suppressed cell cycle-promoting gene expressions in MM cells

The gene ontology analysis based on the microarray-based expression profiling suggested a significant contribution of YAP to the cell cycle process in MM cells. Based on our previous data indicating G1 cell cycle arrest in NCI-H290 cells by YAP knockdown,[17] we studied the status of cell cycle and expressions of cell cycle-promoting genes in a time-dependent manner after YAP-shRNA lentivirus infection. We found that G1 cell cycle arrest occurred at as early as 48 h, and the population of G1 cell cycle arrest increased at 72 h (Figure 3a). With quantitative real-time RT-PCR analysis, suppression of the *CCND1* gene expression was revealed to follow the downregulation of *YAP* as expected (Figure 3c). Consistent with the expression array analysis, other cell cycle-promoting genes including *E2F1, Aurora kinase B* (*AURKB*), *Polo-like kinase 1* (*PLK1*) and *NIMA-related kinase 2* (*NEK2*), also showed the decrease in the expression levels according to YAP-downregulation (Figure 3c). However, other irrelevant genes such as *SMAD3* did not show any decrease (data not shown). These results suggested that, together with YAP-direct target genes of *CCND1* and *FOXM1*, other cell-promoting genes are also involved in the dysregulated cell cycle machinery in YAP-activated MM cells.

Additionally, we observed that YAP-knockdown increased subG1 population of the cells in flow cytometric analysis (Figure 3b) and affected the expression levels of several apoptotic-related genes, including the downregulation of *BIRC5* (also known as *survivin*), an anti-apoptotic gene, and upregulated the one of *BCL2L11* (also known as *BIM*), a pro-apoptotic gene (Supplementary Table 2). In a flow cytometric assay with

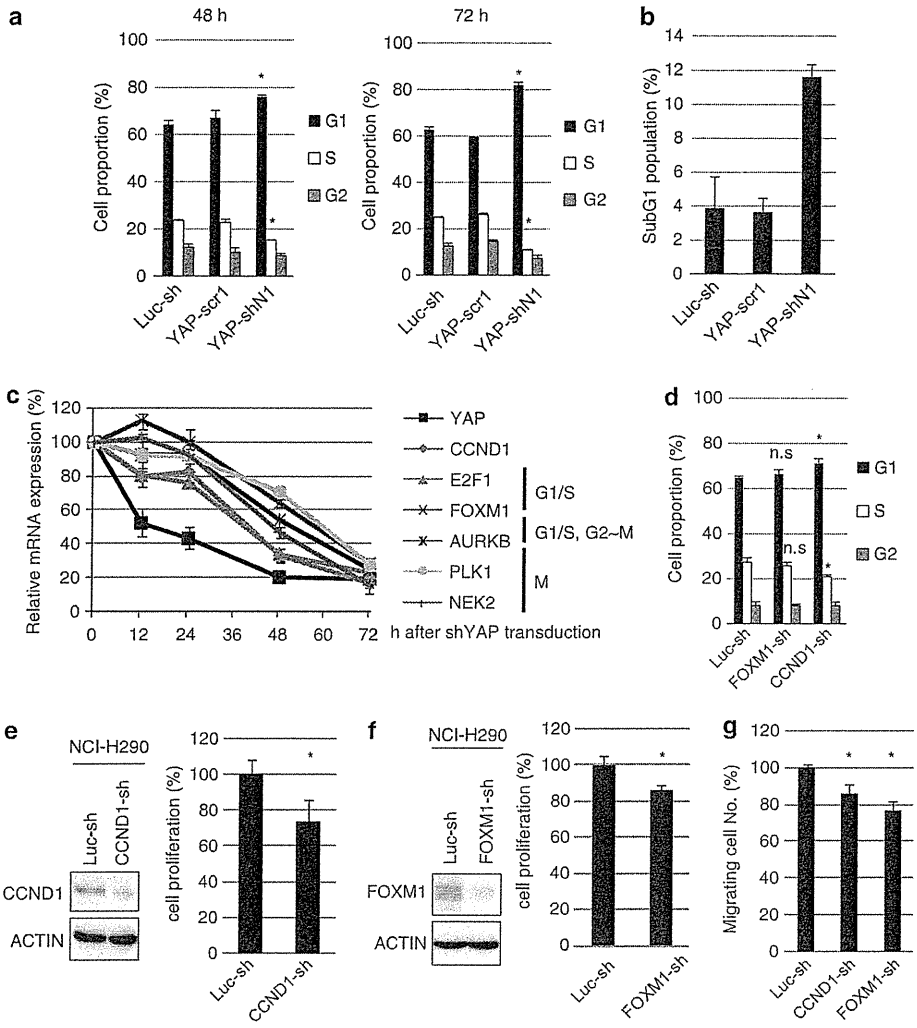

Figure 3. Involvement of YAP, CCND1 and FOXM1 in cell proliferation in NCI-H290 cells. (**a**) Flow cytometry analysis. After infection with YAP-shN1, YAP-scr1, or Luc-sh lentivirus, cells were incubated to grow for 48 or 72 h. Cells were harvested, washed with PBS and fixed with 70% ethanol. After treatment by RNaseA, cells were stained with propidium iodide (Sigma) and flow cytometry analysis was carried out. Cell cycle analysis revealed increased population of G1 phase and decreased population of S phase in NCI-H290 cells 48 h (left) and 72 h (right), respectively, after YAP-shN1 lentivirus infection. (**b**) YAP-knockdown induced subG1 population of MM cells. (**c**) Quantitative real-time RT-PCR analysis was performed with ABI 7500 Real-Time PCR System (Applied Biosystems, Foster, CA, USA). Glyceraldehyde-3-phosphate dehydrogenase (GAPDH) served as an endogenous control. The graph shows the changes in mRNA expression levels of cell cycle-related genes in response to YAP depletion. Symbols are the means of experiments normalized to control cell, and bars represent s.d. (**d**) Flow cytometry analysis. Knockdown of *CCND1* modestly increased the number of G1/S arrest cells in MM cells. (**e**, **f**) Cell proliferation assay. Knockdown of *CCND1* (**e**) and *FOXM1* (**f**) moderately suppressed cell proliferation in NCI-H290 cells. (**g**) Cell migration assay. Knockdown of *CCND1* and *FOXM1* induced modest suppression of NCI-H290 cell migratory activity. Columns are the means of experiments, and bars represent s.d. Asterisks represent $P<0.05$ between YAP-shN1 (**a**), CCND1-sh (**d**, **e**, **g**), or FOXM1-sh (**d**, **f**, **g**) versus Luc-sh control. n.s., not significant.

annexin V, a modest increase of early apoptotic cell population was also detected (Supplementary Figure 2). Although these data suggested apoptosis induction in MM cells, we did not find significant caspase activation with western blot analysis probably due to a relatively small population of MM cells that underwent apoptosis (data not shown). Thus, further studies may be warranted to clarify the underlying mechanism and significance of cell death by YAP-knockdown in MM cells.

CCND1 contributes to G1/S transition in MM cells

To determine whether knockdown of individual cell cycle specific genes regulated by YAP is sufficient to induce G1 cell cycle arrest in MM cells, we performed cell cycle analysis of NCI-H290 cells with knockdown of *CCND1* or *FOXM1*. After transduction of CCND1-sh, we found that the cell population of G1 phase increased and that of S phase decreased compared with the control cell (Figure 3d), although the effect was weaker than that of YAP-sh. However, the effect of FOXM1-sh on cell cycle progression was not clear (Figure 3d).

Finally, to evaluate proliferative roles of CCND1 or FOXM1 as YAP transcriptional targets in MM cells, we knocked down *CCND1* and *FOXM1* and performed proliferation analysis. The depletion of CCND1 and FOXM1 caused modest suppression compared with YAP depletion, though the decrease of proliferation was larger in CCND1 depletion than FOXM1 depletion at 26% and 14%,

respectively (Figures 3e and f). Taken together, these results suggested that YAP contributes to expression of a wide range of cell cycle-promoting genes and induces MM cell proliferation, although knockdown of individual YAP target genes shows moderate effects.

In conclusion, we showed that YAP induces multiple gene expression, which includes cell cycle-promoting genes such as *CCND1* and *FOXM1* in MM cells. Our findings thus serve to elucidate some important aspects of dysregulated cell cycle control mechanisms in MM cells through YAP activation. As individual inhibition of YAP target genes did not suppress MM proliferation sufficiently, we speculate that a wide range of genes evoked by YAP activation induce MM cell proliferation and progression as a whole. Thus, our results suggest that YAP itself may be a key target molecule for the development of a new molecular target therapy for MM.

CONFLICT OF INTEREST

The authors declare no conflict of interest.

ACKNOWLEDGEMENTS

We thank Ms Mika Yamamoto for her excellent technical assistance. This work was supported in part by a Special Coordination Fund for Promoting Science and Technology from the Ministry of Education, Culture, Sports, Science and Technology of Japan (H18-1-3-3-1), KAKENHI (18390245, 22300338), Grant-in-Aid for Third-Term Comprehensive Control Research for Cancer from the Ministry of Health, Labor and Welfare of Japan, the Takeda Science Foundation and the Kobayashi Foundation for Cancer Research.

REFERENCES

1 Pass HI, Vogelzang N, Hahn S, Carbone M. Malignant pleural mesothelioma. *Curr Probl Cancer* 2004; **28**: 93-174.
2 Yang H, Testa JR, Carbone M. Mesothelioma epidemiology, carcinogenesis, and pathogenesis. *Curr Treat Options Oncol* 2008; **9**: 147-157.
3 Robinson BW, Lake RA. Advances in malignant mesothelioma. *N Engl J Med* 2005; **353**: 1591-1603.
4 Vogelzang NJ, Rusthoven JJ, Symanowski J, Denham C, Kaukel E, Ruffie P *et al.* Phase III study of pemetrexed in combination with cisplatin versus cisplatin alone in patients with malignant pleural mesothelioma. *J Clin Oncol* 2003; **21**: 2636-2644.
5 Carbone M, Kratzke RA, Testa JR. The pathogenesis of mesothelioma. *Semin Oncol* 2002; **29**: 2-17.
6 Sekido Y. Genomic abnormalities and signal transduction dysregulation in malignant mesothelioma cells. *Cancer Sci* 2010; **101**: 1-6.
7 Illei PB, Ladanyi M, Rusch VW, Zakowski MF. The use of CDKN2A deletion as a diagnostic marker for malignant mesothelioma in body cavity effusions. *Cancer* 2003; **99**: 51-56.
8 Bianchi AB, Mitsunaga SI, Cheng JQ, Klein WM, Jhanwar SC, Seizinger B *et al.* High frequency of inactivating mutations in the neurofibromatosis type 2 gene (NF2) in primary malignant mesotheliomas. *Proc Natl Acad Sci USA* 1995; **92**: 10854-10858.
9 Sekido Y, Pass HI, Bader S, Mew DJ, Christman MF, Gazdar AF *et al.* Neurofibromatosis type 2 (NF2) gene is somatically mutated in mesothelioma but not in lung cancer. *Cancer Res* 1995; **55**: 1227-1231.
10 Bott M, Brevet M, Taylor BS, Shimizu S, Ito T, Wang L *et al.* The nuclear deubiquitinase BAP1 is commonly inactivated by somatic mutations and 3p21.1 losses in malignant pleural mesothelioma. *Nat Genet* 2011; **43**: 668-672.
11 Testa JR, Cheung M, Pei J, Below JE, Tan Y, Sementino E *et al.* Germline BAP1 mutations predispose to malignant mesothelioma. *Nat Genet* 2011; **43**: 1022-1025.
12 Hamaratoglu F, Willecke M, Kango-Singh M, Nolo R, Hyun E, Tao C *et al.* The tumour-suppressor genes NF2/Merlin and expanded act through Hippo signalling to regulate cell proliferation and apoptosis. *Nat Cell Biol* 2006; **8**: 27-36.
13 Dong J, Feldmann G, Huang J, Wu S, Zhang N, Comerford SA *et al.* Elucidation of a universal size-control mechanism in Drosophila and mammals. *Cell* 2007; **130**: 1120-1133.
14 Saucedo LJ, Edgar BA. Filling out the Hippo pathway. *Nat Rev Mol Cell Biol* 2007; **8**: 613-621.
15 Zhang N, Bai H, David KK, Dong J, Zheng Y, Cai J *et al.* The Merlin/NF2 tumor suppressor functions through the YAP oncoprotein to regulate tissue homeostasis in mammals. *Dev Cell* 2010; **19**: 27-38.
16 Murakami H, Mizuno T, Taniguchi T, Fujii M, Ishiguro F, Fukui T *et al.* LATS2 is a tumor suppressor gene of malignant mesothelioma. *Cancer Res* 2011; **71**: 873-883.
17 Yokoyama T, Osada H, Murakami H, Tatematsu Y, Taniguchi T, Kondo Y *et al.* YAP1 is involved in mesothelioma development and negatively regulated by Merlin through phosphorylation. *Carcinogenesis* 2008; **29**: 2139-2146.
18 Sekido Y. Inactivation of Merlin in malignant mesothelioma cells and the Hippo signaling cascade dysregulation. *Pathol Int* 2011; **61**: 331-344.
19 Huang J, Wu S, Barrera J, Matthews K, Pan D. The Hippo signaling pathway coordinately regulates cell proliferation and apoptosis by inactivating Yorkie, the Drosophila homolog of YAP. *Cell* 2005; **122**: 421-434.
20 Tapon N, Harvey KF, Bell DW, Wahrer DC, Schiripo TA, Haber DA *et al.* Salvador promotes both cell cycle exit and apoptosis in Drosophila and is mutated in human cancer cell lines. *Cell* 2002; **110**: 467-478.
21 Cao X, Pfaff SL, Gage FH. YAP regulates neural progenitor cell number via the TEA domain transcription factor. *Genes Dev* 2008; **22**: 3320-3334.
22 Nishioka N, Inoue K, Adachi K, Kiyonari H, Ota M, Ralston A *et al.* The Hippo signaling pathway components Lats and Yap pattern Tead4 activity to distinguish mouse trophectoderm from inner cell mass. *Dev Cell* 2009; **16**: 398-410.
23 Zhang X, Milton CC, Humbert PO, Harvey KF. Transcriptional output of the Salvador/Warts/Hippo pathway is controlled in distinct fashions in Drosophila melanogaster and mammalian cell lines. *Cancer Res* 2009; **69**: 6033-6041.
24 Zhao B, Ye X, Yu J, Li L, Li W, Li S *et al.* TEAD mediates YAP-dependent gene induction and growth control. *Genes Dev* 2008; **22**: 1962-1971.
25 Hall CA, Wang R, Miao J, Oliva E, Shen X, Wheeler T *et al.* Hippo pathway effector Yap is an ovarian cancer oncogene. *Cancer Res* 2010; **70**: 8517-8525.
26 Muramatsu T, Imoto I, Matsui T, Kozaki K, Haruki S, Sudol M *et al.* YAP is a candidate oncogene for esophageal squamous cell carcinoma. *Carcinogenesis* 2011; **32**: 389-398.
27 Wang Y, Dong Q, Zhang Q, Li Z, Wang E, Qiu X. Overexpression of yes-associated protein contributes to progression and poor prognosis of non-small-cell lung cancer. *Cancer Sci* 2010; **101**: 1279-1285.
28 Xu MZ, Yao TJ, Lee NP, Ng IO, Chan YT, Zender L *et al.* Yes-associated protein is an independent prognostic marker in hepatocellular carcinoma. *Cancer* 2009; **115**: 4576-4585.
29 Zhang X, George J, Deb S, Degoutin JL, Takano EA, Fox SB *et al.* The Hippo pathway transcriptional co-activator, YAP, is an ovarian cancer oncogene. *Oncogene* 2011; **30**: 2810-2822.
30 Basu S, Totty NF, Irwin MS, Sudol M, Downward J. Akt phosphorylates the Yes-associated protein, YAP, to induce interaction with 14-3-3 and attenuation of p73-mediated apoptosis. *Mol Cell* 2003; **11**: 11-23.
31 Lapi E, Di Agostino S, Donzelli S, Gal H, Domany E, Rechavi G *et al.* PML, YAP, and p73 are components of a proapoptotic autoregulatory feedback loop. *Mol Cell* 2008; **32**: 803-814.
32 Levy D, Adamovich Y, Reuven N, Shaul Y. The Yes-associated protein 1 stabilizes p73 by preventing Itch-mediated ubiquitination of p73. *Cell Death Differ* 2007; **14**: 743-751.
33 Anbanandam A, Albarado DC, Nguyen CT, Halder G, Gao X, Veeraraghavan S. Insights into transcription enhancer factor 1 (TEF-1) activity from the solution structure of the TEA domain. *Proc Natl Acad Sci USA* 2006; **103**: 17225-17230.
34 Vassilev A, Kaneko KJ, Shu H, Zhao Y, DePamphilis ML. TEAD/TEF transcription factors utilize the activation domain of YAP65, a Src/Yes-associated protein localized in the cytoplasm. *Genes Dev* 2001; **15**: 1229-1241.
35 Xiao GH, Gallagher R, Shetler J, Skele K, Altomare DA, Pestell RG *et al.* The NF2 tumor suppressor gene product, merlin, inhibits cell proliferation and cell cycle progression by repressing cyclin D1 expression. *Mol Cell Biol* 2005; **25**: 2384-2394.

Supplementary Information accompanies the paper on the Oncogene website (http://www.nature.com/onc)

Interactive CardioVascular and Thoracic Surgery 14 (2012) 560–564
doi:10.1093/icvts/ivr090 Advance Access publication 3 February 2012

INSTITUTIONAL REPORT

Inspiratory capacity as a preoperative assessment of patients undergoing thoracic surgery

Masaki Matsuo[a,†], Naozumi Hashimoto[a,*†], Noriyasu Usami[b], Kazuyoshi Imaizumi[a], Kenji Wakai[c], Tsutomu Kawabe[d], Kohei Yokoi[b] and Yoshinori Hasegawa[a]

[a] Department of Respiratory Medicine, Nagoya University Graduate School of Medicine, Nagoya, Japan
[b] Division of Thoracic Surgery, Nagoya University Graduate School of Medicine, Nagoya, Japan
[c] Department of Preventive Medicine, Nagoya University Graduate School of Medicine, Nagoya, Japan
[d] Department of Medical Technology, Nagoya University Graduate School of Health Science, Nagoya, Japan

* Corresponding author. Department of Respiratory Medicine, Nagoya University Graduate School of Medicine, 65 Tsurumai-cho, Showa-ku, Nagoya 466-8550, Japan. Tel: +81-52-7442167; fax: +81-52-7442176; e-mail: hashinao@med.nagoya-u.ac.jp (N. Hashimoto).

Received 28 July 2011; received in revised form 18 October 2011; accepted 2 November 2011

Abstract

Although inspiratory capacity (IC) is strongly associated with the disease severity of chronic obstructive pulmonary disease, there was no appropriate equation to compute predicted values for IC. Furthermore, whether assessment of IC can identify the risk of prolonged postoperative stay (PPS) in patients undergoing thoracic surgery also remains unclear. To evaluate whether %IC predicted, for which the new equation to compute the predicted values for IC was utilized, could be applied to identify the risk of PPS, we retrospectively analysed the cases of 412 patients who underwent thoracic surgery in Nagoya University Hospital. The multivariate analysis demonstrated that %IC predicted < 85% was one of the most critical risk predictors for PPS (odds ratio, 1.65; 95% confidence intervals, 1.03–2.648) and, in particular, was independent of percentage predicted forced expiratory volume in 1 s (%FEV1) < 80%. A combined assessment of ICFEV1 Low, defined as %IC predicted <85% or %FEV1 <80%, was able to identify more than double the number of patients with PPS, compared with %FEV1 <80% alone (65.9 vs. 28.5%, respectively). This is the first study to demonstrate the significance of %IC predicted in screening for the risk for PPS in patients undergoing thoracic surgery.

Keywords: Chronic obstructive lung disease • Inspiratory capacity • Lung cancer • Screening assessment • Surgical complications

INTRODUCTION

The incidence of chronic obstructive pulmonary disease (COPD) has been increasing considerably among surgical candidates, compared with aged-matched population groups [1]. Since postoperative surgical complications are associated with an enormous economic burden, as a result of patient's unexpected treatments and PPS, we face the urgent need to establish satisfactory preoperative pulmonary assessments.

Progressive symptomatic severity of COPD as well as respiratory failure in COPD patients with acute exacerbation have been demonstrated to be strongly associated with lung hyperinflation, as measured by inspiratory capacity (IC), not forced expiratory volume in 1 s (FEV1) [2]. Although there had been no equations for normal spirometric IC values [3], Tantucci *et al.* [4] demonstrated the importance of %IC to predict the COPD-related mortality, by computing the predicted values for IC in elderly people.

These findings led us to investigate whether IC, measured by spirometry, could be a new predictor to elucidate the risk of PPS in patients undergoing major lung resection, by using the equation to compute the predicted values for IC [4].

PATIENTS AND METHODS

Population

Between 1 January 2006 and 31 December 2009, a total of 422 patients underwent a major pulmonary resection, including pneumonectomy, lobectomy or bilobectomy, in Nagoya University Hospital. Preoperative evaluation for all patients included a detailed history and physical examination, complete blood cell count, serum electrolytes and renal profile, spirometry and a 12-lead electrocardiogram. Preoperative physiological assessments including cardiac assessment and glucose tolerance were also performed and, if necessary, the appropriate treatment for the impairment was performed before surgery. At their first consultation, all patients agreed to stop smoking. Spirometry was performed with a calibrated dry spirometer, a FUDAC-77 (Fukuda Denshi Co., Ltd, Tokyo, Japan), according to American Thoracic Society standards, applied in our hospital [5]. Spirometric variables included vital capacity (VC), residual

† These authors contributed equally to this work.

volume (RV), total lung capacity (TLC), IC, IC/TLC, FEV1, forced vital capacity (FVC), FEV1/FVC and functional residual capacity (FRC). RV, FRC and TLC were assessed with the helium dilution method. Carbon monoxide diffusing capacity (DLCO) and DLCO corrected by the measurement of alveolar volume (VA) (DLCO/VA) were measured by the single breath-holding method. In our hospital, all patients received standardized care in keeping with the clinical practices in use at our institution for in-patients.

Data collection

Data were analysed retrospectively with the approval of the Institutional Review Board of Nagoya University Graduate School of Medicine (No. 27). Individual consent was waived after taking the retrospective nature of the study into account. Preoperative assessment included the documentation of historic information (symptoms, coexistent medical conditions and tobacco use). Data from spirometry, as preoperative pulmonary evaluation, were also collected from the records. Ten patients, who had not undergone preoperative pulmonary assessment by spirometry, were excluded from the study population. Thus, 412 patients constituted the study population.

Pulmonary function variables by spirometry

Airway obstruction was evaluated as the percentage of predicted forced expiratory volume in 1 s (%FEV1) and the percentage of FEV1/FVC. The functional definition of COPD was FEV1/FVC < 70% following the spirometric guidelines of the Global Initiative for Chronic Obstructive Lung Disease (GOLD) [1]. %FEV1 < 80% was defined as '%FEV1 Low'. Predicted values of IC were calculated, using the method described by Tantucci *et al.* [4]. Predicted values of IC for those patients aged <65 or >85 were obtained by back-extrapolating the above-mentioned equations. In this study, %IC predicted < 85% was defined as '%IC Low'. %VC < 80%, %DLCO < 80% and %DLCO/VA < 80% were also defined as '%VC Low', '%DLCO Low' and '%DLCO/VA Low', respectively [6]. To assess the role of the combined evaluation of %IC Low and %FEV1 Low, %IC predicted < 85% or %FEV1 < 80% were defined as 'ICFEV1 Low'.

Postoperative complications and prolonged postoperative stays

The information about postoperative complications before discharge from the hospital was obtained from the hospital records. In this study, the definition of postoperative complications included pulmonary complications and cardiac complications. Postoperative pulmonary complication was evaluated based on the definition of Kroenke *et al.* [7]. Postoperative pulmonary complications included: (i) prolonged oxygen treatment (POT) (the need of oxygen therapy for >2 days or the restart of oxygen therapy); (ii) pneumonia (radiological evidence without bacteriological confirmation was reported as 'pneumonia suspected'; radiological evidence including atelectasis and documentation of pathological organism by Gram stain or culture was reported as 'pneumonia confirmed'; (iii) prolonged ventilation (PV) (unexpected extubation failure at the end of surgery or postoperative ventilator dependence exceeding 48 h); (iv) reintubation due to respiratory failure; and (v) prolonged air leakage [8]. Cardiac complications included myocardial infarction, supraventricular arrhythmias and ventricular arrhythmias, for all of which treatment was needed. Combined cardiac-pulmonary complications included pneumonia, PV, reintubation due to respiratory failure, prolonged air leakage and supraventricular arrhythmias. PPS was defined as a stay of >11 days (11 days was the mean postoperative stay in the non-COPD group).

Statistical analysis

All the collected data were checked for completeness, and the analysed variables were tested for normality of distribution by the Shapiro-Wilk test. Normally distributed variables were compared by the *t*-test and non-normally distributed ones by the Mann-Whitney test between COPD and non-COPD cases or between PPS and non-PPS cases. Comparisons between the proportions were made using the χ^2 test or by the Fisher's exact test. The risk factors found to be predictive of PPS in the above-mentioned univariate analyses were entered into a forward-and-backward stepwise logistic regression analysis to identify independent factors for PPS. All the statistical analyses were done with the PASW Statistics version 18.0 (SPSS Inc., Chicago, IL, USA) and a P value <0.05 was considered statistically significant.

RESULTS

Chronic obstructive pulmonary disease as a risk factor for prolonged postoperative stay and postoperative complications

Patient characteristics are presented in Table 1. A total of 43.2% of the patients undergoing major lung resection had COPD (178/412 cases), only 10% of which were being managed for COPD (18/178 cases). Indeed, most patients with COPD had no or little symptoms, whereas the mean %FEV1 value in the COPD group was significantly lower than that in the non-COPD group (90.47 vs. 111.72%, respectively; $P < 0.0001$). Postoperative stays in the COPD group were significantly longer than that in the non-COPD group (mean: 17 vs. 11 days, respectively; $P = 0.013$). Based on this finding, postoperative stay of >11 days was defined as PPS. The incidence of PPS was significantly higher in the COPD group than in the non-COPD group (45.5 vs. 28.2%, respectively; $P < 0.0001$). The incidence of combined complications was significantly higher in the COPD group than in the non-COPD group (33.7 vs. 19.7%, respectively; $P = 0.003$). The incidence of the POT was significantly higher in the COPD group than in the non-COPD group (39.9 vs. 19.2%, respectively; $P < 0.0001$).

Measurement of inspiratory capacity as a predictor for prolonged postoperative stay

Perioperative historical data and preoperative spirometric data for the patients with or without PPS are summarized in Table 2. POT and combined cardiac-pulmonary complications were closely associated with PPS. Univariate analysis of all patients undergoing major lung resection identified a significantly higher incidence of PPS in men, patients with a history of

Table 1: Patient characteristics and postoperative outcomes among COPD and non-COPD

	Patient characteristics			
	All cases (n = 412)	Non-COPD cases (n = 234)	COPD cases (n = 178)	P value
Age, years[a]	67.1 (31–87)	66.0 (31–87)	68.6 (42–85)	0.001*
Sex, male	293 (71.1)	139 (59.4)	154 (86.5)	0.0001*
History of smoking	316 (76.7)	154 (65.8)	162 (91.0)	0.0001*
COPD	18 (4.3)	3 (1.3)	15 (8.4)	0.0001*
Diabetes	80 (19.4)	47 (20.1)	33 (18.5)	0.694
Ischaemic cardiac disease	38 (9.2)	16 (6.8)	22 (12.4)	0.055
Hypertension	168 (40.8)	93 (39.7)	75 (42.1)	0.453
Neoadjuvant therapy	25 (6.1)	16 (6.8)	9 (5.1)	0.453
BMI, kg m^{-2}[b]	22.2 (3.4)	22.1 (3.8)	22.4 (2.9)	0.745
FEV1/FVC[b]	70.74 (11.3)	78.36 (6.0)	60.85 (8.8)	0.0001*
%FEV1[b]	102.44 (22.5)	111.72 (19.5)	90.47 (20.4)	0.0001*
%IC[b]	89.3 (17.6)	87.44 (17.4)	91.7 (17.7)	0.014*
%IC/TLC[b]	40.86 (7.5)	41.21 (8.1)	40.41 (6.7)	0.277
%VC[b]	108.5 (18.0)	107.00 (17.5)	110.27 (18.5)	0.061
%DLCO[b]	111.7 (29.7)	116.42 (29.1)	105.54 (29.6)	0.017*
%DLCO/VA[b]	95.3 (28.3)	103.4 (26.5)	84.7 (27.2)	0.0001*
Operation time, min[a]	252.3 (44–873)	239.1 (44–604)	269.7 (61–873)	0.002*
Resection				0.663
Pneumonectomy	15 (3.6)	7 (3.0)	8 (4.5)	
Lobectomy	351 (85.2)	202 (86.3)	149 (83.7)	
Others[c]	46 (11.2)	25 (10.7)	21 (11.8)	
Stays, days[a]	13.6 (4–371)	11.0 (4–43)	17.0 (4–371)	0.013*
PPS	147 (35.7)	66 (28.2)	81 (45.5)	0.0001*
POT	116 (28.1)	45 (19.2)	71 (39.9)	0.0001*
Pneumonia	26 (6.3)	11 (4.7)	15 (8.4)	0.123
PV	16 (3.9)	7 (3.0)	9 (5.1)	0.283
Prolonged air leakage	23 (5.6)	9 (3.8)	14 (7.9)	0.078
Supraventricular arrhythmia	53 (12.9)	23 (9.8)	30 (16.9)	0.035*
Combined complication[d]	106 (25.8)	46 (19.7)	60 (33.7)	0.001*

All other data are shown as numbers (%).
PPS: prolonged postoperative stay; POT: prolonged oxygen treatment; PV: prolonged ventilation.
[a]Data are shown as mean (range).
[b]Data are shown as mean (SD).
[c]Others include segmentectomy and wedge resection.
[d]Combined complication; included pneumonia, PV, prolonged air leakage and supraventricular arrhythmia.
*$P < 0.05$.

smoking, patients with COPD (FEV1/FVC < 70%), %FEV1 Low, %IC Low, %VC Low, %DLCO Low or %DLCO/VA Low, longer operation time, operating methods and neoadjuvant therapy for lung cancer. All these factors were applied to the multivariate model to identify the perioperative variables independently associated with PPS. The multivariate analysis identified %IC Low, %FEV1 Low and operation time as independent risk factors for the development of PPS (Table 3). Although %FEV1 Low identified <30% of the patients with PPS (42/147 cases), %IC Low was able to identify 52.4% of the patients with PPS (77/147 cases). Finally, to evaluate whether combined assessment of %IC and %FEV1 could identify the patients with PPS, the assessment of ICFEV1 Low was applied to the study population. It was shown that ICFEV1 Low could identify >65% of the patients with PPS (97/147 cases), indicating that ICFEV1 Low might be able to identify the patients at risk of PPS, through the use of spirometry as a screening assessment.

DISCUSSION

Regardless of early efforts to develop perioperative pulmonary risk indices, preoperative pulmonary assessment has not been so well developed as cardiac assessment [6]. Physical examination findings have been assumed to be more helpful in assessing the magnitude of risk than spirometry [9], whereas most patients undergoing major lung resection have little or no symptoms and abnormal physiological finding. Nevertheless, our data demonstrated that the patients with COPD (defined as FEV1/FVC < 70%) experienced a 61% increase in average PPS, a 100% increase in POT and a 71% increase in the incidence of combined cardiac–pulmonary complications, compared with those without COPD. In the present study, the other comorbidities including diabetes, ischaemic cardiac diseases and hypertension were not associated with the development of PPS in these patients, indicating that the standardized perioperative management for these comorbidities could prevent PPS and postoperative complications [6, 9]. Although a recent report suggests that spirometry should not be used to screen for airflow obstruction in individuals without respiratory symptoms [9], our data suggested that early detection of COPD patients with no or little symptom might contribute to prevent prolonged hospital stays in the patients undergoing thoracic surgery.

Because decreased ventilatory lung volume and atelectasis may be the first events in a cascade leading to postoperative

Table 2: Patient characteristics and postoperative outcomes among PPS and non-PPS

	Patient characteristics			
	All cases (n = 412)	Non-PPS cases (n = 265)	PPS cases (n = 147)	P value
Age, years[a]	67.1 (31–87)	66.9 (35–87)	67.4 (31–85)	0.583
Sex, male	293 (71.1)	177 (66.8)	116 (78.9)	0.001*
History of smoking	316 (76.7)	187 (70.6)	129 (87.8)	<0.0001*
COPD	18 (4.3)	10 (3.8)	8 (5.4)	0.694
Diabetes	80 (19.4)	48 (18.1)	32 (21.8)	0.088
Ischaemic cardiac disease	38 (9.2)	23 (8.7)	15 (11.4)	0.43
Hypertension	168 (40.8)	110 (39.5)	58 (39.5)	0.488
Neoadjuvant therapy	25 (6.1)	13 (4.3)	12 (11.1)	0.002*
BMI, kg m^{-2}[b]	22.2 (3.4)	22.3 (3.3)	22.0 (3.7)	0.374
FEV1/FVC < 70% (COPD)	178 (43.2)	97 (36.6)	81 (55.1)	<0.0001*
%FEV1 Low	60 (14.6)	18 (6.8)	42 (28.5)	<0.0001*
%IC Low	168 (40.8)	91 (34.3)	77 (52.4)	<0.001*
%IC/TLC[c]	40.89 (7.5)	41.3 (7.6)	40.06 (7.3)	0.112
%VC Low	19 (4.6)	7 (2.6)	12 (8.2)	<0.0001*
%DLCO Low	64 (15.5)	26 (9.8)	38 (26.5)	<0.0001*
%DLCO/VA Low	120 (29.1)	61 (23.0)	59 (40.1)	<0.0001*
Operation time, min[a]	252.3 (44–873)	224.4 (44–459)	302.6 (101–873)	<0.0001*
Resection				0.001*
Pneumonectomy	15 (3.6)	3 (1.1)	12 (8.2)	
Lobectomy	351 (85.2)	229 (86.4)	122 (83.0)	
Others[d]	46 (11.2)	33 (12.5)	13 (8.8)	
Stays, days[a]	13.6 (4–371)	9.2 (4–11)	21.7 (12–371)	<0.0001*
POT	116 (28.1)	45 (17.0)	71 (48.3)	<0.0001*
Pneumonia	26 (6.3)	3 (1.1)	23 (15.6)	<0.0001*
PV	16 (3.9)	2 (0.7)	14 (9.5)	<0.0001*
Prolonged air leakage	23 (5.6)	3 (1.1)	20 (13.6)	<0.0001*
Supraventricular arrhythmia	53 (12.9)	18 (6.8)	20 (13.6)	<0.0001*
Combined complication[e]	106 (25.8)	29 (10.9)	79 (53.7)	<0.0001*

All other data are shown as numbers (%).
PPS: prolonged postoperative stay; POT: prolonged oxygen treatment; PV: prolonged ventilation.
[a]Data are shown as mean (range).
[b]COPD are managed as COPD patients and shown as numbers (%).
[c]Data are shown as mean (SD).
[d]Others include segmentectomy and wedge resection.
[e]Combined complication; included pneumonia, PV, prolonged air leakage and supraventricular arrhythmia.
*P < 0.05.

Table 3: Multivariate analysis of risk factors for PPS

Variables	Odds ratio	95% CI	P value
%IC Low (<85% vs. 85%)	1.65	1.029–2.648	0.038*
%FEV1.0 Low (<80% vs. 80%)	3.90	2.003–7.597	<0.0001*
Operation time (per 1 min)	1.01	1.006–1.012	<0.0001*

PPS: prolonged postoperative stay.
*P < 0.05.

pulmonary complications for all patients undergoing a surgical operation [10], tidal volume and respiratory rate have been assumed to be helpful variables, not only to predict the need of mechanical ventilation after pneumonectomy, but also to assess readiness to wean and the timing of extubation from mechanical ventilation [11]. Recent studies on the association of the disease severity of COPD with the IC have elucidated a strong statistical correlation between these two parameters in COPD [12]. Therefore, we evaluated whether IC, measured by spirometry, could be applied to the elucidation of the risk of PPS in patients undergoing major lung resection.

Our multivariable analysis indicated that '%IC Low' was the most critical and independent risk predictor for PPS among all the estimated variables besides '%FEV1 Low'. Although ERS/ESTS clinical guideline recommended the combined assessment of %FEV1 and %DLCO as screening in the patients undergoing thoracic surgery [6], our data showed the limited ability of %FEV1 predicted < 80% and %DLCO < 80% as risk screening. Our data suggested that there was only small difference in %DLCO between non-PPS cases and PPS cases (117.0 vs. 102.1%, respectively). Although the incidence of PPS reached 70% (42/60) in the patients with %FEV1 predicted < 80%, <30% of the patients with PPS (42/147 cases) were detected by %FEV1 Low. In contrast, '%IC Low' could identify 52.4% of the patients with PPS (77/147 cases). Furthermore, the combined assessment of ICFEV1 Low was shown to identify more than double the number of patients with PPS (66.0%; 97/147 cases), compared with %FEV1 Low alone. These data indicated that as a screening assessment, IC

Low and/or ICFEV1 Low are more appropriate than FEV Low, although the specificity was lower in the former. Assessment of IC value measured by spirometry has a clear limitation in that the accurate measurement of lung volume can only be adequately performed with body plethysmograph [3]. Nevertheless, our analysis suggested that %IC measurement and combined assessment of ICFEV1 Low using spirometry might have two major benefits for elucidating the risk of PPS in the patients undergoing thoracic surgery. One is that these screening assessments allow enough time to arrive at a decision on the most appropriate treatments for lower pulmonary function. The other is that, because body plethysmograph is an expensive and inconvenient procedure, only a few institutions have this facility. Therefore, there are practical objections to measuring IC by this method. In contrast, as most hospitals and institutions have spirometry, the measurement of IC by spirometry will be easy to implement and on quite a large scale [4]. Finally, a further investigation into the validity of %IC measurement for the population of patients with major lung resection is warranted.

AUTHOR CONTRIBUTIONS

N.H. had full access to all of the data in the study and takes responsibility for the integrity of the data and the accuracy of the data analysis. Study concept and design: N.H. Acquisition of data: M.M. and N.H. Analysis and interpretation of data: M.M., N.H., N.U., K.I., K.W., T.K., K.Y. and Y.H. Drafting of the manuscript: N.H. Critical revision of the manuscript for important intellectual content: K.Y. and Y.H. Statistical analysis: N.H. and K.W.

Conflict of interest: none declared.

REFERENCES

[1] Rabe KF, Hurd S, Anzueto A, Barnes PJ, Buist SA, Calverley P *et al.* Global strategy for the diagnosis, management, and prevention of chronic obstructive pulmonary disease: GOLD executive summary. Am J Respir Crit Care Med 2007;176:532–55.

[2] Stevenson NJ, Walker PP, Costello RW, Calverley PM. Lung mechanics and dyspnea during exacerbations of chronic obstructive pulmonary disease. Am J Respir Crit Care Med 2005;172:1510–6.

[3] Casanova C, Cote C, de Torres JP, Aguirre-Jaime A, Marin JM, Pinto-Plata V *et al.* Inspiratory-to-total lung capacity ratio predicts mortality in patients with chronic obstructive pulmonary disease. Am J Respir Crit Care Med 2005;171:591–7.

[4] Tantucci C, Donati P, Nicosia F, Bertella E, Redolfi S, De Vecchi M *et al.* Inspiratory capacity predicts mortality in patients with chronic obstructive pulmonary disease. *Respir Med 2008;102:613–9.*

[5] Pellegrino R, Viegi G, Brusasco V, Crapo RO, Burgos F, Casaburi R *et al.* Interpretative strategies for lung function tests. Eur Respir J 2005;26: 948–68.

[6] Brunelli A, Charloux A, Bolliger CT, Rocco G, Sculier JP, Varela G *et al.* ERS/ESTS clinical guidelines on fitness for radical therapy in lung cancer patients (surgery and chemo-radiotherapy). Eur Respir J 2009;34:17–41.

[7] Kroenke K, Lawrence VA, Theroux JF, Tuley MR. Operative risk in patients with severe obstructive pulmonary disease. Arch Intern Med 1992;152:967–71.

[8] Sekine Y, Behnia M, Fujisawa T. Impact of COPD on pulmonary complications and on long-term survival of patients undergoing surgery for NSCLC. Lung Cancer 2002;37:95–101.

[9] Qaseem A, Wilt TJ, Weinberger SE, Hanania NA, Criner G, van der Molen T *et al.* Diagnosis and management of stable chronic obstructive pulmonary disease: a clinical practice guideline update from the American College of Physicians, American College of Chest Physicians, American Thoracic Society, and European Respiratory Society. Ann Intern Med 2011;155:179–91.

[10] Lawrence VA, Cornell JE, Smetana GW. Strategies to reduce postoperative pulmonary complications after noncardiothoracic surgery: systematic review for the American College of Physicians. Ann Intern Med 2006; 144:596–608.

[11] Boles J-M, Bion J, Connors A, Herridge M, Marsh B, Melot C *et al.* Weaning from mechanical ventilation. Eur Respir J 2007;29:1033–56.

[12] O'Donnell DE, Banzett RB, Carrieri-Kohlman V, Casaburi R, Davenport PW, Gandevia SC *et al.* Pathophysiology of dyspnea in chronic obstructive pulmonary disease: a roundtable. Proc Am Thorac Soc 2007;4:145–68.

Activated Leukocyte Cell-Adhesion Molecule (ALCAM) Promotes Malignant Phenotypes of Malignant Mesothelioma

Futoshi Ishiguro, MD,† Hideki Murakami, MD, PhD,* Tetsuya Mizuno, MD,*† Makiko Fujii, DDS, PhD,* Yutaka Kondo, MD, PhD,* Noriyasu Usami, MD, PhD,† Kohei Yokoi, MD, PhD,† Hirotaka Osada, MD, PhD,*‡ and Yoshitaka Sekido, MD, PhD*‡*

Introduction: Cell-adhesion molecules play important roles involving the malignant phenotypes of human cancer cells. However, detailed characteristics of aberrant expression status of cell-adhesion molecules in malignant mesothelioma (MM) cells and their possible biological roles for MM malignancy remain poorly understood.

Methods: DNA microarray analysis was employed to identify aberrantly expressing genes using 20 MM cell lines. Activated leukocyte cell-adhesion molecule (ALCAM) expression in MM cell lines was analyzed with quantitative reverse transcription-polymerase chain reaction and Western blot analyses in 47 primary MM specimens with immunohistochemistry. ALCAM knockdown in MM cell lines was performed with lentivirus-mediated short hairpin RNA (shRNA) transduction. Purified soluble ALCAM (sALCAM) protein was used for in vitro experiments, whereas MM cell lines infected with the sALCAM-expressing lentivirus were tested for tumorigenicity in vivo.

Results: ALCAM, a member of the immunoglobulin superfamily, was detected as one of the most highly upregulated genes among 103 cell-adhesion molecules with microarray analysis. Elevated expression levels of ALCAM messenger RNA and protein were detected in all 20 cell lines. Positive staining of ALCAM was detected in 26 of 47 MM specimens (55%) with immunohistochemistry. ALCAM knockdown with shRNA suppressed cell migration and invasion of MM cell lines. Purified sALCAM protein impaired the migration and invasion of MM cells in vitro, and the infection of sALCAM-expressing virus into MM cells significantly prolonged survival periods of MM-transplanted nude mice in vivo.

Conclusion: Our study suggests that overexpression of ALCAM contributes to tumor progression in MM and that ALCAM might be a potential therapeutic target of MM.

Key Words: Activated leukocyte cell-adhesion molecule (ALCAM), Malignant mesothelioma, Migration, Invasion, Soluble isoform.

(*J Thorac Oncol.* 2012;7: 890–899)

Malignant mesothelioma (MM) is an aggressive tumor arising from mesothelial cells of the pleural or peritoneal cavity, and exposure to asbestos is considered to play a crucial role in tumor development.[1–5] Despite advances in the chemotherapeutical modalities combining cisplatin and antifolate agent such as pemetrexed[6] or the trials of radical multimodal therapy including neoadjuvant chemotherapy followed by extrapleural pneumonectomy and hemithoracic radiation,[7–9] the prognosis of patients with MM remains very poor. New approaches to the treatment are needed to improve their outcome.

Aberrant expressions of cell-adhesion molecules in cancer cells play important roles in cell proliferation, migration, and metastasis.[10,11] As for cell-adhesion molecules associated with MM, positivity of N-cadherin or CD141 and negativity of E-cadherin or CD15 have been proposed to be useful diagnostic findings for the epithelial type of MM.[12] Recently, CD146 has been proposed as an immunocytochemical marker for differential diagnosis of MM from reactive mesothelium.[13] However, only a few reports have aimed to resolve the relationship between aberrant expression of cell-adhesion molecules and MM progression.[14–16]

Activated leukocyte cell-adhesion molecule (ALCAM/CD166) is a type-I transmembrane protein and a member of the immunoglobulin superfamily.[17,18] ALCAM comprises five extracellular immunoglobulin-like molecules (D1–D5), a transmembrane domain, and a short COOH-terminal cytoplasmic tail (Supplementary Figure 1A, Supplemental Digital Content 1, http://links.lww.com/JTO/A259).[19] ALCAM was first identified on activated leukocytes as a ligand of CD6,[20,21] and ALCAM-CD6-mediated adhesion was shown to contribute

*Division of Molecular Oncology, Aichi Cancer Center Research Institute, Nagoya, Japan; †Division of Thoracic Surgery, Nagoya University Graduate School of Medicine, Nagoya, Japan; and ‡Department of Cancer Genetics, Program in Function Construction Medicine, Nagoya University Graduate School of Medicine, Nagoya, Japan.

Address for correspondence: Yoshitaka Sekido, MD, PhD, Division of Molecular Oncology, Aichi Cancer Center Research Institute, 1-1 Kanokoden, Chikusa-ku, Nagoya, Aichi 464–8681, Japan. E-mail: ysekido@aichi-cc.jp

Disclosure: This work was supported in part by a Special Coordination Fund for Promoting Science and Technology from the Ministry of Education, Culture, Sports, Science and Technology of Japan (H18-1-3-3-1), grants-in-aid for Scientific Research (B) from the Japan Society for the Promotion of Science (18390245, 22300338), a grant-in-aid for Third-Term Comprehensive Control Research for Cancer from the Ministry of Health, Labor and Welfare of Japan, the Takeda Science Foundation, and the Kobayashi Foundation for Cancer Research. The authors declare no conflict of interest.

ISSN: 1556-0864/12/890-899

to T-cell activation or proliferation.[22,23] Meanwhile, ALCAM was also demonstrated to mediate homophilic ALCAM-to-ALCAM interaction,[24,25] which was shown to be involved in physiological processes including angiogenesis,[26] immune response,[27] and cell migration during the neuronal development.[28] As for carcinogenesis, ALCAM has been reported to participate in the promotion of cell migration or invasion in vitro[29,30] and the enhancement of tissue invasion and metastases in vivo.[31] In primary malignant tumors, overexpression of ALCAM has also been demonstrated to be pathologically correlated with aggressiveness in colorectal cancer,[32] gastric cancer,[33] and various types of cancers.[34–39]

Meanwhile, a soluble isoform of ALCAM (sALCAM) has also been identified as an alternative, shortened ALCAM transcript.[26] This transcript contains only one of the five immunoglobulin domains, D1, which was shown to be the most important region for ligand binding (Supplementary Figure 1C, Supplemental Digital Content 1, http://links.lww.com/JTO/A259).[25] sALCAM was shown to block homophilic binding of ALCAM, and was considered to have a regulatory role in blocking endogenous ALCAM function.[27] Moreover, sALCAM was also demonstrated to inhibit tumor progression; sALCAM treatment impaired melanoma cell migration in vitro and diminished metastatic properties in vivo.[31]

In this study, we found ALCAM to be one of the most upregulated genes among cell-adhesion molecule-encoding genes in MM cell lines and showed the overexpression of ALCAM in more than half of MM primary tumors. We showed that ALCAM knockdown by short hairpin RNA (shRNA) exerted inhibitory effects on cell migration and invasion of MM cells. Furthermore, we demonstrated that the sALCAM attenuated the malignant phenotypes of MM cells in vitro and that a xenographic murine model inoculated with MM cells that were infected with sALCAM-expressing lentivirus showed a prolonged survival. Our results indicate that ALCAM has a significant role in MM cell progression and that ALCAM may well be a molecular target against MM cells.

MATERIALS AND METHODS

Cell Lines and Primary Specimens of MM

Fourteen Japanese MM cell lines, including ACC-MESO-1, -4, Y-MESO-8D, -9, -12, -14, -21, -22, -25, -26B, -27, -28, -29, and -30, were established in our laboratory as reported previously and described elsewhere, and the cells at 10 to 15 passages were used for assays.[40] Four MM cell lines including NCI-H28, NCI-H2052, NCI-H2373, and MSTO-211H, and one immortalized mesothelial cell line, MeT-5A, were purchased from the American Type Culture Collection (ATCC) (Rockville, MD), and cells at 3 to 5 passages were used. NCI-H290 and NCI-H2452 were the kind gift of Dr. Adi F. Gazdar. All MM cell lines were cultured in RPMI1640 medium supplemented with 10% fetal calf serum and 1× antibiotic-antimycotic (Invitrogen, Carlsbad, CA) at 37°C in a humidified incubator with 5% CO_2. MeT-5A was cultured according to ATCC instructions. Two primary cultures of normal mesothelial cells at 3 to 5 passages derived from ascites of patients with ovarian cancer, OV-M1, gastric cancer, GAS-M1, were also used. Forty-seven primary specimens of MMs used included 35 pleura, 6 peritoneum, and 6 other sites of origins. Histological classification was 34 epithelial, 6 biphasic, 5 spindle, 1 desmoplastic, and 1 lymphohistiocytoid. Among 47 MMs, 28 were MM tissue samples obtained from patients at Aichi Cancer Center Hospital, Nagoya University Hospital, Japanese Red Cross Nagoya First Hospital, Toyota Kosei Hospital, and Kasugai Municipal Hospital according to the Institutional Review Board-approved protocol of each and the written informed consent from each patient. Fifteen primary MM samples were obtained as result of biopsy, 11 samples via extrapleural pneumonectomy and 2 samples were collected via pleurectomy/decortication. Overall survival was measured from the date of surgery until death or the final date of the follow-up. The median length of follow-up for patients was 12 months (range, 2–38 months). Normal lung samples were obtained from patients with lung cancer who had undergone curative pulmonary resection. The other 19 MM samples were from the human mesothelioma tissue array from US Biomax (Rockville, MD).

Antibodies

Mouse anti-ALCAM antibody (clone MOG/07 and SNCL-CD166) for Western blot and immunohistochemical analysis was purchased from Novocastra (Newcastle, U.K.). Mouse anti-ALCAM (clone 3A6, 559260) for immunofluorescence was purchased from BD Bioscience Discovery Labware (Bedford, MA) and mouse anti-β-actin (clone AC74) was from Sigma (St. Louis, MO). Rabbit anti-β-catenin antibody (sc-7199) was purchased from Santa Cruz Biotechnology (Santa Cruz, CA), and mouse anti-V5 was from Invitrogen.

Construction of RNA Interference Vectors and Expression Vectors

Complementary short hairpin (sh) sequence was cloned into pLentiLox3.7[41] under control of a U6 promoter and transfected into HEK293FT cells along with the vectors of VSVG, RSV-Rev, and pMDLg-pRPE, to generate lentiviruses that transcribe shRNA. Two sh oligonucleotides were designed for two different sequences within the ALCAM open reading frame (ALCAM-Sh1, 5′-GAGGAATCTCCTTATATTA-3′ and ALCAM-Sh2, 5′-GGATAACATCACTCTTAAA-3′). Control vectors, ALCAM-Scr1 (5′-GTTTACCACGGAATATTAT-3′) and ALCAM-Scr2 (5′-GAAACCTTTTCAGCAATAA-3′) were constructed using oligonucleotides with scrambled sequence for ALCAM-Sh1 and ALCAM-Sh2. The efficacy of each virus was tested by immunoblotting of whole cell lysates 96 hours after infecting NCI-H290 cells at the multiplicity of infection of 10. The cDNA fragments of wild-type ALCAM or sALCAM were amplified by PCR using PrimeSTAR Max DNA polymerase (Takara Bio, Otsu, Japan), and introduced into the pcDNA3.1 V5-His expression vector (Invitrogen), thereby fusing these cDNAs with the V5-His sequence. The sequences of all constructs were confirmed. To generate wild-type ALCAM- or sALCAM-expressing lentiviral vectors, cDNA coding for ALCAM or sALCAM tagged with V5-His was amplified with PCR and cloned into the pLL3.7Lox

lentiviral vector with an infusion cloning system (Clontech, Mountain View, CA).

Purification of sALCAM

HEK293FT cells were infected with V5-His-tagged sALCAM-expressing or empty virus as a control. Ninety-six hours after infection, the media were exchanged to serum-free medium and cells were incubated for 24 hours. The conditioned media were collected and subjected to purification of sALCAM using the His-tagged protein purification kit (Qiagen K.K., Tokyo, Japan). Purified His-tagged proteins were dialysed to remove buffer-containing imidazole and sodium using Biotech Cellulose Ester membranes (Spectrum Laboratories, Rancho Dominguez, CA). Then, proteins were filtrated at a concentration of 20-fold using Amicon Ultra-0.5 devices (Millipore, Bedford, MA).

Animals and Implantation Model

Female KSN/Slc nude mice (nu/nu) were obtained from Japan SLC (Hamamatsu, Japan) and maintained under specific pathogen-free conditions throughout this study. NCI-H290 cells either infected with sALCAM-V5- or GFP-lentivirus were harvested using trypsin/EDTA, washed twice, and suspended in phosphate-buffered saline. Six-week-old mice were injected with 1×10^6 cells in 100 μl of PBS into the right thoracic cavity. Survival was measured from the date of injection of MM cells until death. All experiments were performed in accordance with the guidelines established by the Aichi Cancer Center Committee on Animal Care and Use.

Additional materials and methods are described in Supplementary Material and Methods (Supplemental Digital Content 2, http://links.lww.com/JTO/A260).

RESULTS

ALCAM Expression in MM Cell Lines and Primary Tissues

To determine what types of cell-adhesion molecules are aberrantly expressed in MM cells, we performed microarray analysis using 20 MM cell lines. Among 103 genes that encode cell-adhesion molecules from the array, we listed the top 10 genes that showed either up- or downregulation in MM cells (Supplementary Table 1, Supplemental Digital Content 3, http://links.lww.com/JTO/A261). Because ALCAM was the second- highest scoring gene and has been reported to be associated with other types of human malignancies, we focused on ALCAM for its roles in the pathogenesis of MM. To validate the microarray data, we next examined the expression status of ALCAM with quantitative reverse transcription-polymerase chain reaction and Western blot analyses. Comparing with the expression level of ALCAM mRNA in an immortalized mesothelial cell line, MeT-5A, which was arbitrarily set as 1.0, all 20 cell lines expressed more than 4.5-fold ALCAM mRNA, with 15 cell lines being more than 20-fold (Fig. 1*A*). Meanwhile, two primary cell cultures of normal mesothelial cells, OV-M1, and GAS-M1, also showed relatively low expression of ALCAM. Western blot analysis also confirmed increased ALCAM protein in all 20 cell lines, which seemed to be consistent with mRNA expression levels (Fig. 1*B*). Each MM cell line expressed ALCAM of different sizes. The different sizes of ALCAM were thought to be not only because of different posttranslational modifications of the ALCAM protein such as glycosylation, but also because of splice variants (variant 1, 2, and 3) of the *ALCAM* gene, with the estimated molecular weight of each being 65.1, 63.6, and 61.9 kDa, respectively.[19] We also performed immunocytochemical analysis using NCI-H290 cells and observed strong signals at cell-to-cell interaction regions (Fig. 1*C*). However, ALCAM signals in MeT-5A cells were undetectable (Fig. 1*C*).

To study whether ALCAM expression detected in MM cell lines reflects primary MMs, we investigated ALCAM expression in 47 MM specimens with immunohistochemical analysis. We detected 9 specimens (19%) for 3+, 17 (36%) for 2+, 14 (30%) for 1+, and 7 (15%) for 0 score, indicating that 26 of 47 specimens (55%) were positive (3+ or 2+) for ALCAM. As five specimens were the origins of cell lines, we compared them and found that four pairs of cell lines and primary tumors (Y-MESO-9/KD1048, Y-MESO-12/KD1050, Y-MESO-14/KD1053, and Y-MESO-21/KD1056) showed a well-concordant expression of ALCAM (Figs. 2*A–D*). Although the Y-MESO-26B cell line showed a high expression of ALCAM, its corresponding primary specimen, KD1062, showed faint staining (1+) of ALCAM (Fig. 2*E*). Meanwhile, normal pleural mesothelial cells also showed faint staining (1+) (Fig. 2*F*). We investigated the relationship between the ALCAM immunohistochemical staining status and clinicopathological characteristics of MMs. However, there was no significant relationship between ALCAM expression and the sites of origin or histological subtypes (Supplementary Table 2, Supplemental Digital Content 4, http://links.lww.com/JTO/A262). Survival data of 22 patients were also available from 28 of our patients. However, we did not detect a significant association between the ALCAM expression and the patients' survival (data not shown).

Inhibition of ALCAM-Suppressed Migration and Invasion of Mesothelioma Cells

As ALCAM is reportedly involved in the promotion of tumor cell migration and invasion in other types of human malignancies, we investigated whether or not inhibition of ALCAM suppresses malignant phenotypes of MM cells. We selected H290 and Y-MESO-27 as representative cell lines with high and moderate ALCAM protein expression, respectively. We synthesized two ALCAM shRNA constructs and confirmed ALCAM-Sh1 suppressed ALCAM protein expression more efficiently than ALCAM-Sh2 in two mesothelioma cell lines (Fig. 3*A*). Using these ALCAM-Sh constructs, we found that ALCAM knockdown induced 30 to 50% inhibition of cell migration and invasion of both cell lines (Fig. 3*B*). We further carried out colony formation assay and found that ALCAM knockdown also impaired anchorage-independent cell growth (Fig. 3*C*). However, we did not detect the inhibitory effect on cell proliferation by ALCAM knockdown (Supplementary Figure 2, Supplemental Digital Content 5, http://links.lww.com/JTO/A263).

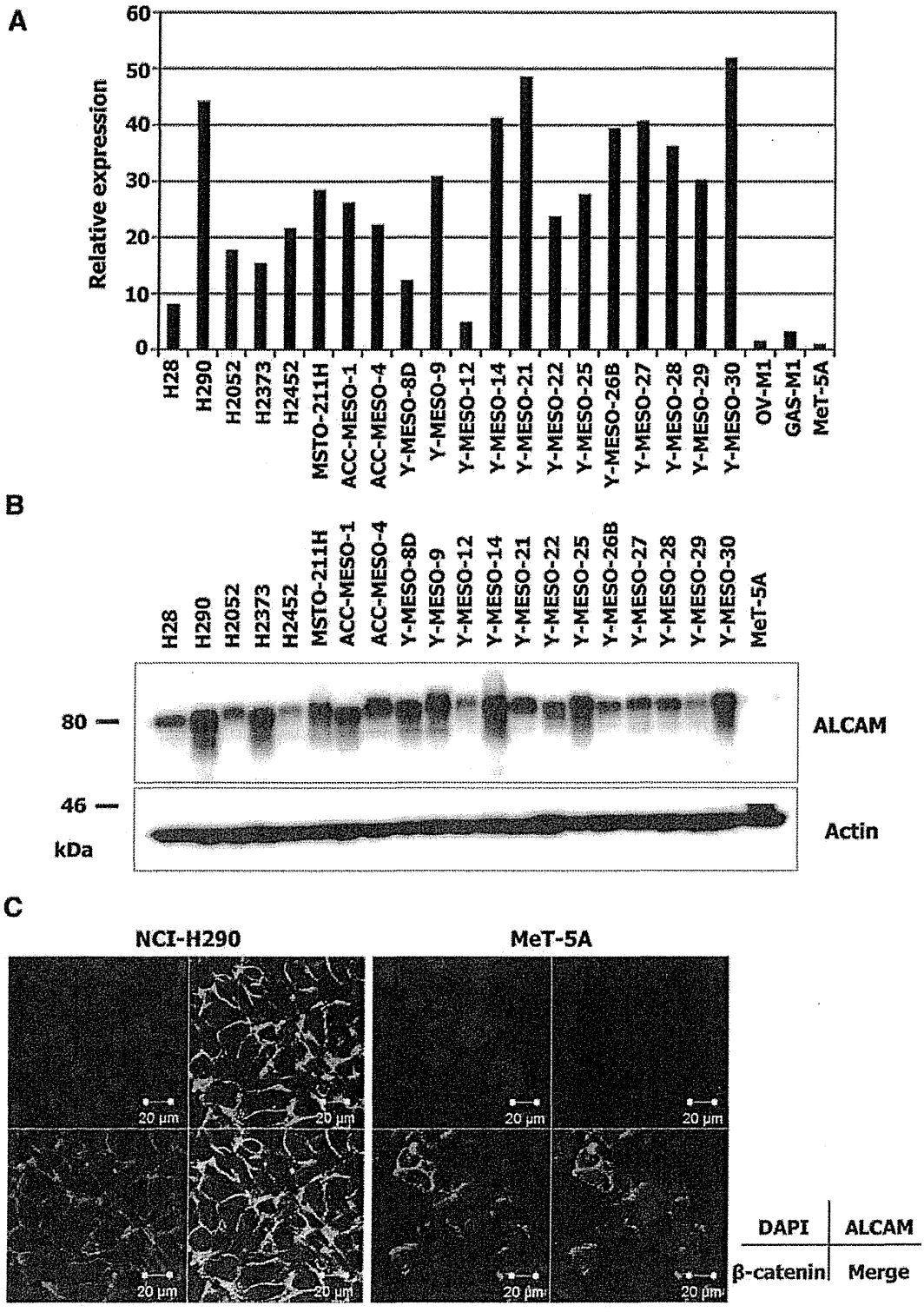

FIGURE 1. Expression of ALCAM in MM cell lines. (*A*) Quantitative RT-PCR analysis of ALCAM in 20 MM cell lines, 1 immortalized cell line, MeT-5A, and 2 primary normal mesothelial cultures, OV-M1 and GAS-M1. Relative expression of MeT-5A was arbitrarily set at 1.0, (*B*) Western blot analysis of ALCAM in 20 MM cell lines. Expression of β-actin was used as the control, (*C*) Immunocytochemical analysis. Strong, membranous signals of ALCAM were observed in NCI-H290 cells, but no signals in MeT-5A cells. β-catenin staining was used as the marker of the cell-to-cell interaction region. ALCAM, Activated leukocyte cell-adhesion molecule; MM, malignant mesothelioma; RT-PCR, reverse transcription polymerase chain reaction.

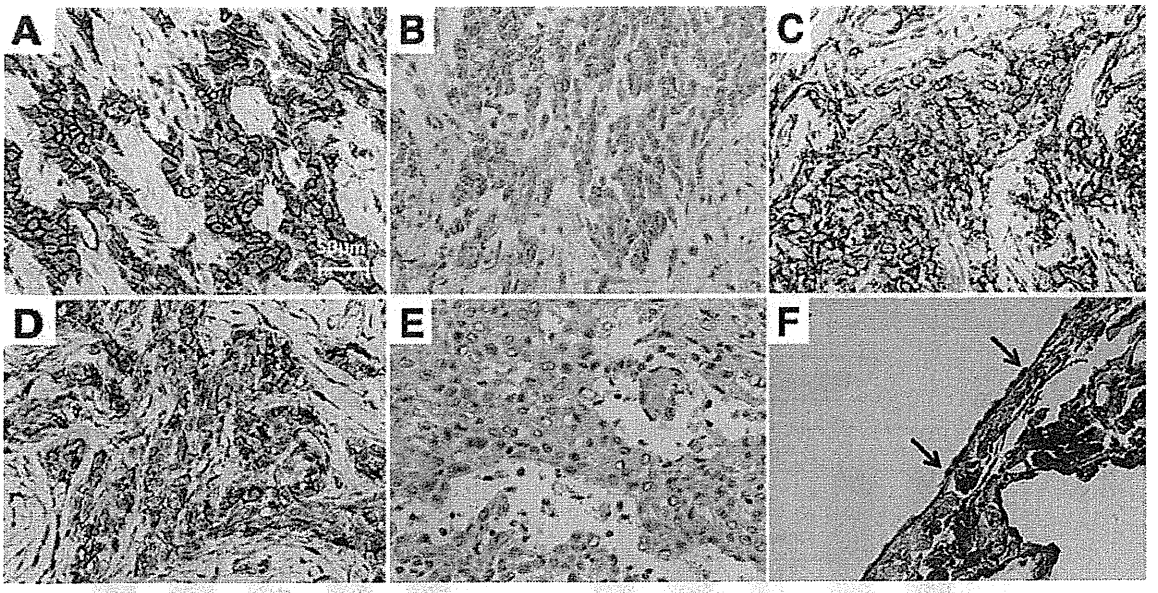

FIGURE 2. Immunohistochemical analysis of ALCAM in primary MM specimens. ALCAM was positive in KD1048 (3+) (*A*), KD1050 (2+) (*B*), KD1053 (3+) (*C*), and KD1056 (3+) (*D*). These samples were the origins of Y-MESO-9 cell line (20.2 for relative ALCAM mRNA level), Y-MESO-12 (4.7), Y-MESO-14 (35.2), and Y-MESO-21 (51.6), respectively, as shown in Figure 1*A*. Although KD1062 showed faint staining (1+) (*E*), its corresponding cell line, Y-MESO-26B, showed high ALCAM expression (30.4). Normal pleural mesothelial cells (arrows) (*F*) showed faint staining (1+) of ALCAM. ALCAM, Activated leukocyte cell-adhesion molecule; MM, malignant mesothelioma; mRNA, messengerRNA.

ALCAM Induces Enhancement of Migration and Anchorage-Independent Growth of Normal Mesothelial Cells

To determine whether ALCAM confers malignant phenotypes to normal mesothelial cells, we infected the wild-type ALCAM virus into MeT-5A cells (Fig. 4*A*). With immunocytochemical analysis, we confirmed that ectopically expressed ALCAM was localized at the cell-to-cell interaction regions (Fig. 4*B*). We found that the transduction of ALCAM increased cell migration and anchorage-independent cell growth of MeT-5A cells (Fig. 4*C*). However, we could not observe the enhancement of cell invasion ability (data not shown). As expected, we did not detect promotion of MeT-5A cell proliferation with enhanced ALCAM expression (Supplementary Figure 3, Supplemental Digital Content 6, http://links.lww.com/JTO/A264); this suggested that ALCAM does not affect cell proliferation itself as seen in ALCAM-knockdown MM cells.

Regulatory Effect of sALCAM on ALCAM Function

To evaluate a possible inhibitory effect of the soluble form, sALCAM (Supplementary Figure 1C, Supplemental Digital Content 1, http://links.lww.com/JTO/A259), on MM cells we generated sALCAM expression virus with V5-epitope tag that was attached at the COOH-terminal, and infected HEK293FT cells with them to synthesize sALCAM protein. With Western blot analysis using anti-V5 antibody, sALCAM was detected in the cell lysates and conditioned culture medium of HEK293FT/sALCAM-V5 cells (Fig. 5*A*). We then purified the His-tagged sALCAM protein from conditioned culture medium, and the purity was confirmed by silver staining (Fig. 5*B*). We added sALCAM in the culture medium of MM cell lines and found that sALCAM induced 20 to 40% inhibition of cell migration and invasion of MM cells (Fig. 5*C*). We further demonstrated that purified sALCAM significantly impaired anchorage-independent cell growth of MM cells (Fig. 5*D*). However, we did not observe any inhibitory effect of sALCAM on cell proliferation (Supplementary Figure 5, Supplemental Digital Content 1, http://links.lww.com/JTO/A265).

Survival Benefit of sALCAM in MM Cell-Bearing Nude Mice

To assess the possible therapeutic effect of sALCAM in vivo, we infected NCI-H290 cells with sALCAM-expressing virus and injected them into the right thoracic cavity of nude mice. We found that nude mice inoculated with the MM cell line with sALCAM expression, NCI-H290/sALCAM-V5, exhibited significantly prolonged survival time, compared with the control, NCI-H290/GFP (Fig. 6). Autopsy using Western blot and immunohistochemical analyses served to confirm stable expression of sALCAM in the thoracic tumors (Supplementary Figure 5, Supplemental Digital Content 8, http://links.lww.com/JTO/A266).

DISCUSSION

In the present study, we found that ALCAM is one of the most highly upregulated genes among cell adhesion-related genes in MM cells and that ALCAM gives a malignant phenotype to MM cells. We showed elevated expression of

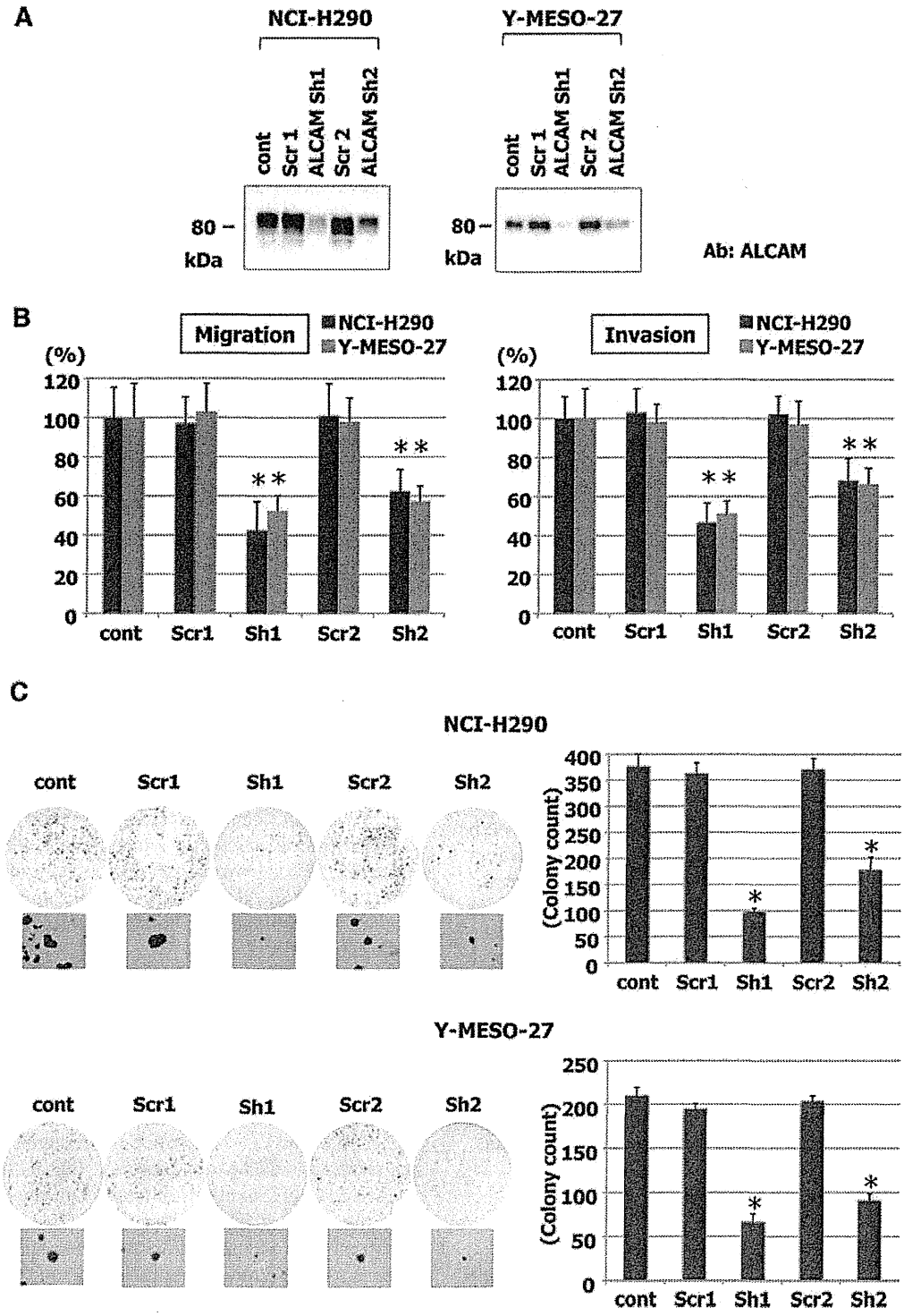

FIGURE 3. Lentiviral shRNA-mediated ALCAM knockdown in two MM cell lines, NCI-H290 and Y-MESO-27. (*A*) Western blot analysis demonstrates efficiency of ALCAM knockdown. Both ALCAM-Sh vectors, ALCAM Sh1 and ALCAM Sh2, showed effective suppression of the level of ALCAM protein, whereas the control vectors, ALCAM Scr1 and ALCAM Scr2, showed no inhibition. Cells were lysed 96 hours after infection. (*B*) ALCAM knockdown inhibited migration and invasion of two MM cell lines. (*C*) Inhibition of ALCAM with shRNA-mediated knockdown in MM cell lines suppressed anchorage-independent colony formation. Representative results of the NCI-H290 and Y-MESO-27 cell lines are shown (top) with higher magnifications of their representative colonies (bottom). The results of the triplicate experiments are presented. Columns, mean; bars, SD. ALCAM, Activated leukocyte cell-adhesion molecule; MM, malignant mesothelioma; shRNA, short hairpin RNA. *$p < 0.05$ vs. control.